ISTANBUL TECHNICAL UNIVERSITY ★ GRADUATE SCHOOL

AIRCRAFT TRAJECTORY OPTIMIZATION UNDER WIND EFFECT BY USING OPTIMAL CONTROL: ENVIRONMENTAL IMPACT ASSESSMENT

M.Sc. THESIS

Fulin SEZENOĞLU

Department of Defence Technologies

Defence Technologies Programme

NOVEMBER 2022

ISTANBUL TECHNICAL UNIVERSITY ★ GRADUATE SCHOOL

AIRCRAFT TRAJECTORY OPTIMIZATION UNDER WIND EFFECT BY USING OPTIMAL CONTROL: ENVIRONMENTAL IMPACT ASSESSMENT

M.Sc. THESIS

Fulin SEZENOĞLU
(514191047)

Department of Defence Technologies

Defence Technologies Programme

Thesis Advisor: Prof. Dr. İbrahim ÖZKOL

NOVEMBER 2022

İSTANBUL TEKNİK ÜNİVERSİTESİ ★ LİSANSÜSTÜ EĞİTİM ENSTİTÜSÜ

OPTİMAL KONTROL İLE RÜZGAR ETKİSİ ALTINDA UÇAK ROTA OPTİMİZASYONU VE HAVACILIĞIN ÇEVRE ÜZERİNDEKİ ETKİSİNİN İNCELENMESİ

YÜKSEK LİSANS TEZİ

Fulin SEZENOĞLU
(514191047)

Savunma Teknolojileri Anabilim Dalı

Savunma Teknolojileri Programı

Tez Danışmanı: Prof. Dr. İbrahim ÖZKOL

KASIM 2022

Fulin SEZENOĞLU, a M.Sc. student of İTU Graduate School student ID 514191047, successfully defended the thesis entitled "AIRCRAFT TRAJECTORY OPTIMIZATION UNDER WIND EFFECT BY USING OPTIMAL CONTROL: ENVIRONMENTAL IMPACT ASSESSMENT", which she prepared after fulfilling the requirements specified in the associated legislations, before the jury whose signatures are below.

Thesis Advisor : **Prof. Dr. İbrahim ÖZKOL** ....
Istanbul Technical University

Jury Members : **Assoc. Prof. Emre KOYUNCU** ....
Istanbul Technical University

Prof. Dr. Osman Ergüven VATANDAŞ ....
Istanbul Gelişim University

Date of Submission : 21 October 2022
Date of Defense : 11 November 2022

FOREWORD

This master thesis is written to complete M.Sc. program at Istanbul Technical University. The aircraft trajectory optimization under wind effect by using optimal control and environmental impact assessment is studied within this thesis. This master thesis is supported by European Union's Horizon 2020 research and innovation programme under grant agreement No 875503, project ClimOP (Climate Assessment of Innovative Mitigation Strategies Towards Operational Improvements in Aviation).

During process of my thesis, I would like to express my gratitude and respect to my advisor Prof. Dr. İbrahim ÖZKOL who guided me with his immense knowledge, experience and motivation. I would also like to thank my family whose moral support I have always felt.

Also, I would like to thank Asst. Prof. Barış BAŞPINAR for his support throughout this thesis.

October 2022 Fulin SEZENOĞLU
(Software Developer)

TABLE OF CONTENTS

Page

FOREWORD……………………………………………………………………..vii
TABLE OF CONTENTS…………………………………………………......ix
ABBREVIATIONS…………………………………………………………xi
SYMBOLS…………………………………………………………………..xiii
LIST OF TABLES……………………………………………………...xv
LIST OF FIGURES…………………………………………………..........xvii
SUMMARY…………………………………………………………......xix
ÖZET……………………………………………………………………xxiii
1. INTRODUCTION.. 1
1.1 Scope of Thesis 3
1.2 Literature Review 3
1.3 Thesis Structure 6
2. PROBLEM FORMULATION... 7
2.1 General Form of Optimal Control Problem.. 7
2.2 Optimal Control Solution Techniques.. 7
2.2.1 Dynamic programming methods 8
2.2.2 Indirect methods 8
2.2.3 Direct methods.. 9
2.3 Constraints.. 9
2.4 Optimization Problem 10
2.5 Solving Optimal Control Problem.. 11
3. WIND-WEATHER OPTIMIZED TRAJECTORY GENERATION 13
3.1 Assumptions 14
3.2 Atmosphere Model 14
3.2.1 Determination of air pressure and temperature... 14
3.2.2 Determination of air density 15
3.2.3 Determination of Mach number... 15
3.2.4 The standard atmosphere model parameters... 16
3.3 Aircraft Dynamics 16
3.3.1 2D aircraft model 17
3.3.2 3D aircraft model 17
3.4 Aircraft Performance Model... 18
3.4.1 BADA 3 aircraft performance parameters.. 19
3.4.1.1 Aerodynamics 19
3.4.1.2 Engine thrust 20
3.4.1.3 Fuel consumption.. 20
3.4.2 BADA 4 aircraft performance parameters... 21
3.4.2.1 Aerodynamics 21
3.4.2.2 Engine thrust 22
3.4.2.3 Fuel consumption.. 23
3.5 Wind Model.. 24

3.5.1 Data preprocessing 26
3.5.2 Multiple regression analysis 28
3.6 Emission Model 30
4. SIMULATION AND RESULTS 35
4.1 Case Study 1: The Investigation of Turkish Airspace Specific to Istanbul to Ankara Flights 35
4.1.1 Problem setup 35
4.1.2 Wind data 35
4.1.3 Numerical results 37
4.1.3.1 Fuel consumption 39
4.1.3.2 Travel time 39
4.1.3.3 NO_x and CO_2 emissions 39
4.2 Case Study 2: The Investigation of European Airspace Specific to Paris to Frankfurt Flights 39
4.2.2 Wind data 40
4.2.3 Numerical results 41
4.2.3.1 Fuel consumption 43
4.2.3.2 Travel time 43
4.2.3.3 NO_x and CO_2 emissions 43
5. CONCLUSION 45
REFERENCES 47
CURRICULUM VITAE 51

ABBREVIATIONS

AEM3	: Advanced Emission Model 3
AGTP	: Absolute Global Temperature Potential
AML	: Algebraic Modelling Language
APM	: Aircraft Performance Model
ARPM	: Airline Procedure Model
ATM	: Air Traffic Management
ATR	: Average Temperature Response
BADA	: Base of Aircraft Data
BM2	: Boeing Method 2
CGD	: Charles de Gaulle Airport
CO	: Carbon monoxide
CO_2	: Carbon dioxide
DoF	: Degree of Freedom
DLR	: German Aerospace Center
EDDF	: Frankfurt Airport
EoM	: Equation of Motion
GFS	: Global Forecast System
GRIB	: Gridded Binary
FRA	: Frankfurt Airport
HC	: Hydrocarbon
H_2O	: Oxygen Hydride
ICAO	: International Civil Aviation Organization
IPOPT	: Interior Point Optimizer
ISA	: International Standard Atmosphere
LFPG	: Charles de Gaulle Airport
LTAC	: Ankara Esenboğa Airport
LTBA	: Istanbul Atatürk Airport
LTO	: Landing and Takeoff
MSL	: Mean Sea Level
NCEP	: National Centers for Environmental Prediction
NLP	: Nonlinear Programming Problem
NO_x	: Nitrogen Oxide
PFM	: Propulsive Forces Model
PMM	: Point Mass Model
SO_x	: Sulphur Oxides
TBO	: Trajectory Based Operations

SYMBOLS

a	: Speed of sound
$a_{1:36}$	: Non-idle rating thrust coefficients
A	: Scaling factor
$\beta_{T,<}$	: Lapse rate
c_1, c_2, c_3	: Objective function coefficients
C_L&C_D	: Lift & Drag coefficients
C_F&C_T	: Fuel & Thrust coefficients
CO_2	: Carbondioxide
$d_{1:15}$	: Clean drag coefficients
$EINO_x$	: Emission indices of NO_x
g_0	: Gravitational acceleration
$f_{1:25}$	: Non-idle rating fuel coefficients
F	: Fuel consumption
t	: Time
u	: Control input
x(t)	: State variable
h	: Altitude
H_P	: Geopotential pressure altitude
m	: Mass
M	: Mach number
NO_x	: Nitrogen oxides
p	: Path vector
P	: Pressure
P_0	: Standard atmospheric pressure at MSL
R	: Real gas constant
S	: Wing reference area
κ	: Adiabatic index
ψ	: Heading angle
ϕ	: Bank angle
γ	: Flight path angle
δ	: Thrust lever position
δ_{amb}	: Ambient pressure ratio
δ_P	: Pressure ratio
δ_T	: Throttle parameter
θ	: Temperature ratio
θ_{amb}	: Ambient temperature ratio
ρ	: Air density
x, y	: Horizontal position
x_e&y_e&z_e	: Longitude&Latitude&Altitude
v	: True airspeed
T	: Temperature
Thr	: Thrust force

$\mathbf{T_0}$	**:** Standard atmospheric temperature at MSL
$\boldsymbol{W}$	**:** Wind speed
$\boldsymbol{W_{m_{ref}}}$	**:** Weight force at reference mass

LIST OF TABLES

Page

Table 3.1: The standard atmosphere model parameters based on BADA 4. 16
Table 4.1: Optimization and flight plan results for Istanbul to Ankara flights on October 6, 2018.. 38
Table 4.2: The optimization and flight plan results for Paris to Frankfurt flights on October 6,2018.. 42

LIST OF FIGURES

Sayfa

Figure 1.1 : The wind-weather optimized aircraft trajectory optimization framework **2**
Figure 3.1 : The flowchart of wind-weather optimized trajectory generation **13**
Figure 3.2 : The structure of BADA model **19**
Figure 3.3 : The wind field of European Airspace for a different barometric altitudes **25**
Figure 3.4 : The data smoothing of horizontal wind components (in m/s) on October 1, 2018. The upper plots are for x component of wind (real wind data has shown on the left and smoothed data has shown on the right) and the lower plots are for y components of wind (real wind data has shown on the left and smoothed data has shown on the right)........ **25**
Figure 3.5 : The data smoothing of horizontal wind components (in m/s) on October 5, 2018. The upper plots are for x component of wind (real wind data has shown on the left and smoothed data has shown on the right) and the lower plots are for y components........ **27**
Figure 3.6 : The data smoothing of horizontal wind components (in m/s) on October 7, 2018. The upper plots are for x component of wind (real wind data has shown on the left and smoothed data has shown on the right) and the lower plots are for y components........ **28**
Figure 3.7 : The regression analyses of horizontal wind components (in m/s) on October 1, 2018 at 150 [HPa] barometric altitude........ **29**
Figure 3.8 : The regression analyses of horizontal wind components (in m/s) on October 5, 2018 at 100 [HPa] barometric altitude........ **30**
Figure 3.9 : The regression analyses of horizontal wind components (in m/s) on October 7, 2018 at 350 [HPa] barometric altitude........ **30**
Figure 3.10 : Fuel calculation cycle of the AEM3........ **31**
Figure 3.11 : Fuel burn and emission calculations for AEM3........ **32**
Figure 4.1 : The data smoothing of meridional and zonal wind components (in m/s) at 300 [HPa] barometric altitude. The upper plots are for x component of wind (real wind data has shown on the left and smoothed data has shown on the right) and the lower plots are for y components........ **36**
Figure 4.2 : The magnitude of meridional (left) and zonal(right) wind components at 300 [HPa] indicates real wind forecasts (dots) and analytical functions (surfaces)........ **36**
Figure 4.3 : The wind-weather optimized trajectory for İstanbul – Ankara cruise flight........ **37**
Figure 4.4 : The data smoothing of meridional and zonal wind components (in m/s) at 300 [HPa] barometric altitude. The upper plots are for x component of wind (real wind data has shown on the left and smoothed data has shown on the right) and the lower plots are for y components........ **40**

Figure 4.5 : The magnitude of meridional and zonal wind components at 150 [HPa] shows real wind forecasts (blue dots) and analytical functions (surfaces) **40**
Figure 4.6 : The wind-weather optimized trajectory for Paris – Frankfurt cruise flight………………………………………………………………..**41**

AIRCRAFT TRAJECTORY OPTIMIZATION UNDER WIND EFFECT BY USING OPTIMAL CONTROL: ENVIRONMENTAL IMPACT ASSESSMENT

SUMMARY

The aim of this thesis, Aircraft Trajectory Optimization Under Wind by Using Optimal Control and Environmental Impact of Aviation in terms of Aircraft Emissions, is to find the wind and weather optimized aircraft trajectories in the cruise phase by minimizing fuel consumption, time and air pollutants. Flight trajectories calculated by taking into account the wind factor are considered as a critical measure in terms of reducing fuel consumption. In addition, it is known that the models examined by including weather information give more realistic results than those that are not included. Trajectory planning calculations consist of various elements such as wind forecasts, operational constraints, amount of fuel, aircraft performance, atmospheric conditions. Temperature, pressure and air density parameters are considered standard atmospheric values. The performance model used is based on BADA.

In order to achieve the aims of the thesis, first of all, the problem has been tried in 2 dimensions in terms of reducing complexity of operations. At this stage, the wind equation, which was created with a simple calculation, was added to the EoM in horizontal plane. The effect of the horizontal components of wind is clearly seen in the numerical simulation. Secondly, the problem was created according to BADA 3 and solved in a way that minimizes flight time and fuel in 3 dimensional space. Simultaneously, a wind model has been created with the wind tabular data obtained from the Global Forecast System (GFS). The GFS is a weather forecast model developed by the National Centers for Environmental Prediction (NCEP). In this study, wind factor was assumed to be stationary, wind uncertainty was not included in this study. Since there are erroneous measurements in the wind tabular data obtained from the Global Forecasting System (GFS), the data was improved by applying the interpolation method first and the error difference between the real data and the interpolated data was arranged to be the least. Then, with the smooth data, wind equations were obtained separately for seven barometric altitude levels. Thirdly, in addition to flight time and fuel consumption, an emission model was created based on the ICAO Engine Exhaust Data Bank [29] and Boeing Method 2 [30] to solve the multi-objective optimization problem. The developed new model was applied to the simulation environment created based on BADA 4. Finally, the wind equations in the horizontal plane obtained were included in the simulation environment developed on the basis of BADA 4, and the targeted model was created.

Predetermined routes were filtered from the actual flight plan selected for the same day with the wind data to be examined in the case studies. The flight area was determined and a wind model was obtained for that region. All one-day flights for the selected route were examined. Wind equations are calculated by taking flight hours into account. The simulation results were obtained according to the flight information

of the desired route obtained from the real flight plan. The optimized trajectories were calculated in the simulation environment by referring to the points where the aircraft started and ended the cruise phase. Thus, Turkish airspace, which has not been examined before, is presented as a case study specific to Istanbul-Ankara flights. As a second case study, European airspace is presented specific to Paris-Frankfurt flights. During these studies, it was clearly seen that cruising speed and cruising altitude are critical for fuel consumption under the wind effect. In addition, as a result of these studies, it has been shown that the proposed model gives more effective results as the flight distance increases.

This study consists of five chapters describing the stages of the thesis.

The first chapter is a general introduction to the thesis topic. The thesis topic is explained and its aims are mentioned, the importance of the subject and why it is needed are presented. This section consists of three sub-titles. First of all, the scope and contributions of the thesis are mentioned. Afterwards, a wide literature review was made and studies in this field were presented. Finally, the structure of the thesis is mentioned.

In the second chapter, the mathematical model required for this study is explained. Wind-optimized trajectories for an aircraft in the cruise phase are generated by solving a non-linear optimal control problem. For this reason, first of all, the general representation of the optimal control problem and its solution techniques are mentioned. The suitability of these solution techniques to the problem is discussed and the method to solve the problem is explained. It is known that multi-objective optimization problems give more realistic and ideal results than single-objective optimization problems. After this part, multi-objective optimization problem and constraints are defined. In the last part, the optimal control problem solution method is mentioned. GEKKO Python optimization module was used for numerical simulation in solving the aircraft trajectory optimization problem. This algorithm was developed to analyze the environmental impact of emitted aircraft emissions such as nitrogen oxides and carbon dioxide, using real air traffic data.

In the third chapter, models used in trajectory generation optimized for wind and weather conditions are introduced. First, the assumptions are mentioned. Afterwards, the atmosphere model, aircraft performance model, wind model and emission model are explained in detail. In addition, the equations of motion of the aircraft in 2D and 3D are shown in this section.

In the fourth chapter, two case studies on the subject and their results are presented. First of all, it is the main contribution to the literature to analyze the flights over Turkey, which has not been focused on before as a case study. First, the problem is defined in the case analysis. Then, the wind field over the Turkish airspace was examined and a wind model was created. The wind equations of the region, which was extracted to include Istanbul and Ankara, were obtained and added to the equations of motion of an aircraft, as explained in wind model section in third chapter. In the simulation environment created in this direction, the most optimized trajectories were calculated considering the Istanbul-Ankara flights. As the second case study, Paris-Frankfurt flights over European airspace were analyzed. As in the first application, after defining the problem respectively and examining the wind field covering the flight points, the multi-objective optimization problem was solved for this route. As a result of the case studies, the actual and calculated flight time, fuel consumption, NOx and CO2 emission findings for each flight are presented comparatively.

In the fifth and also the last chapter, the results and other studies that can be done in this field are mentioned. The values obtained as a result of the case analyzes are emphasized again. Within the scope of the study, it has been shown that the adverse impacts of aviation on the climate are reduced by trajectory optimization, which is resolved by evaluating wind and environmental effects. The topics that can be studied on the basis of this study in the future are mentioned.

OPTİMAL KONTROL İLE RÜZGAR ETKİSİ ALTINDA UÇAK ROTA OPTİMİZASYONU: HAVACILIĞIN ÇEVRESEL ETKİSİNİN DEĞERLENDİRİLMESİ

ÖZET

Optimal Kontrol ile Rüzgar Etkisi Altında Uçak Rota Optimizasyonu ve Havacılığın Uçak Emisyonları Bakımından Çevreye Etkisinin İncelenmesi yüksek lisans mezuniyet tezinin amacı, yakıt tüketimi, zaman ve hava kirleticilerini minimize ederek, rüzgar ve hava durumuna göre optimize edilmiş seyir fazındaki en iyilenmiş uçak rotalarını bulmaktır. Rüzgar faktörü dikkate alınarak hesaplanan uçuş rotaları, yakıt tüketimini azaltmak açısından ciddi bir önlem olarak kabul edilir. Ayrıca, hava durumu bilgisi dahil ederek incelenen modellerin, dahil edilmeyenlere göre daha gerçekçi sonuçlar verdiği bilinmektedir. Rota planlama hesaplamaları, rüzgar tahminleri, operasyonel kısıtlar, yakıt miktarı, uçak performansı, atmosferik koşullar gibi çeşitli unsurlardan oluşur. Sıcaklık, basınç ve hava yoğunluğu parametreleri standart atmosfer değerleri olarak kabul edilir. Kullanılan performans modeli BADA'ya dayanmaktadır.

Tezin amaçlarına ulaşmak adına öncelikle işlem kolaylığı açısından problem 2 boyutta denenmiştir. Bu aşamada basit bir hesaplamayla oluşturulan rüzgar denklemi yatay düzlemdeki hareket denklemlerine eklenmiştir. Rüzgarın yatay bileşenlerinin etkisi nümerik simülasyonda açıkça görülmüştür. İkinci olarak, problem BADA 3'e göre oluşturulup, 3 boyutta uçuş süresini ve yakıtı minimize edecek şekilde çözülmüştür. Eş zamanlı olarak Küresel Tahmin Sistemi (GFS)'nden elde edilen rüzgar tablo verileri ile rüzgar modeli oluşturulmaya başlanmıştır. Küresel Tahmin Sistemi (GFS), Ulusal Çevresel Tahmin Merkezleri (NCEP) tarafından geliştirilen bir hava tahmini modelidir. Bu çalışmada rüzgar durağan kabul edilmiştir, rüzgar belirsizliği bu çalışma kapsamında dahil edilmemiştir. Küresel Tahmin Sistemi (GFS)'nden elde edilen rüzgar tablo verileri içerisinde hatalı ölçümler bulunduğundan öncelikle interpolasyon yöntemi uygulanarak veriler iyileştirilmiş ve gerçek veri ile interpole edilmiş veri arasındaki hata farkı en az olacak şekilde düzenlenmiştir. Daha sonra, düzenlenmiş veri ile rüzgar denklemleri yedi barometrik irtifa değeri için ayrı ayrı elde edilmiştir. Üçüncü olarak, uçuş süresi ve yakıt tüketimine ek olarak, çok amaçlı optimizasyon problemini çözmek için ICAO Motor Egzoz Veri Bankası [29] ve Boeing Metot 2 [30] esas alınarak emisyon modeli oluşturulmuştur. Geliştirilen yeni model, BADA 4 temel alınarak oluşturulan simülasyon ortamına uygulanmıştır. Son olarak, elde edilen yatay düzlemde rüzgar denklemleri de BADA 4 temel alınarak geliştirilen simülasyon ortamına dahil edilerek hedeflenen model oluşturulmuştur.

Rüzgar verisi ile aynı gün için seçilen gerçek uçuş planından, vaka analizinde incelenmek üzere önceden belirlenen rotalar filtrelenmiştir. Uçuş yapılan alan çıkartılıp, o bölge için rüzgar modeli elde edilmiştir. Seçilen rota için bir günlük bütün uçuşlar incelenmiştir. Rüzgar denklemleri uçuş saatleri dikkate alınarak hesaplanmıştır. Gerçek uçuş planından elde edilen istenilen rotaya ait uçuş bilgilerine

göre simülasyon sonuçları elde edilmiştir. Uçağın seyir fazına başladığı ve bitirdiği noktalara referans alınarak simülasyon ortamında en iyilenmiş rotalar hesaplanmıştır. Böylelikle daha önce incelenmemiş Türkiye hava sahası, İstanbul-Ankara uçuşları özelinde vaka analizi olarak sunulmuştur. İkinci bir vaka analizi olarak, Avrupa hava sahası, Paris-Frankfurt uçuşları özelinde sunulmuştur. Bu çalışmalar sırasında, seyir hızının ve seyir irtifasının, rüzgar etkisi altında yakıt tüketimi açısından kritik önem taşıdığı açıkça görülmüştür. Ayrıca bu çalışmaların sonucunda, önerilen modelin uçuş mesafesi arttıkça daha etkili sonuçlar verdiği gösterilmiştir.

Bu çalışma, tezin aşamalarını anlatan beş bölümden oluşmaktadır.

Birinci bölüm tez konusuna genel bir giriş niteliğindedir. Tez konusu açıklanıp amaçlarından bahsedilmiştir, konunun önemi ve neden ihtiyaç duyulduğu sunulmuştur. Bu bölüm, üç alt başlıktan oluşmaktadır. İlk olarak tezin kapsamı ve katkılarından bahsedilmiştir. Daha sonra geniş bir literatür taraması yapılarak bu alanda yapılan çalışmalar sunulmuştur. Son olarak ise tezin yapısından bahsedilmiştir.

İkinci bölümde bu çalışma için gerekli olan matematiksel model anlatılmıştır. Seyir fazındaki uçaklar için rüzgara göre optimize edilmiş rotalar, doğrusal olmayan bir optimal kontrol problemi çözülerek üretilir. Bunun sebeple, öncelikli olarak optimal kontrol probleminin genel gösterimi ve çözüm tekniklerinden bahsedilmiştir. Bu çözüm tekniklerinin probleme uygunlukları tartışılıp, problemin nasıl bir yöntemle çözüleceği anlatılmıştır. Çok amaçlı optimizasyon problemlerinin, tek amaçlı optimizasyon problemlerine göre daha gerçekçi ve ideal sonuçlar verdiği bilinmektedir. Bu kısımdan sonra çok amaçlı optimizasyon problemi ve kısıtlar tanımlanmıştır. Son kısımda ise optimal kontrol problemi çözüm yönteminden bahsedilmiştir. Uçak rota optimizasyonu probleminin çözümünde nümerik simülasyon için GEKKO Python optimizasyon modülü kullanılmıştır. Bu algoritma, gerçek hava trafik verileri kullanılarak, nitrojen oksit ve karbondioksit gibi salınan uçak emisyonlarının çevre üzerindeki etkisini analiz etmek için geliştirilmiştir.

Üçüncü bölümde rüzgara ve hava durumuna göre optimize edilmiş rota hesaplamada kullanılan modeller tanıtılmıştır. İlk olarak yapılan kabullerden bahsedilmiştir. Sonrasında atmosfer modeli, uçak performans modeli, rüzgar modeli ve emisyon modeli detaylı olarak anlatılmıştır. Ayrıca bu bölümde 2 boyutta ve 3 boyutta uçağın hareket denklemleri gösterilmiştir.

Dördüncü bölümde, konu ile ilgili iki tane vaka analizi ve sonuçları sunulmuştur. Öncelikle, vaka incelemesi olarak daha önce odaklanılmamış olan Türkiye üzerindeki uçuşlardan hareketle analizlerin yapılması literatüre yapılan katkılardandır. İlk olarak vaka analizinde problem tanımlanmıştır. Daha sonra Türkiye hava sahası üzerindeki rüzgar alanı incelenmiş ve rüzgar modeli oluşturulmuştur. İstanbul ve Ankara'yı içine alacak şekilde çıkartılan bölgenin rüzgar denklemleri, üçüncü bölümde rüzgar modeli kısmında anlatıldığı üzere, elde edilerek uçağın hareket denklemlerine eklenmiştir. Bu doğrultuda oluşturulan simülasyon ortamında, İstanbul-Ankara uçuşları dikkate alınarak en iyilenmiş rotalar hesaplanmıştır. İkinci vaka analizi olarak ise Avrupa hava sahası üzerinde Paris-Frankfurt uçuşları analiz edilmiştir. İlk uygulamada olduğu şekilde, sırasıyla problem tanımlanıp, uçuş noktalarını kapsayan rüzgar alanı incelendikten sonra çok amaçlı optimizasyon problemi bu rota için çözülmüştür. Vaka analizleri sonucunda, her uçuş için gerçekte olan ve hesaplanan uçuş süresi, yakıt tüketimi, NO_x ve CO_2 emisyonu bulguları karşılaştırmalı olarak sunulmuştur.

Beşinci ve son bölümde, sonuçlar ve bu alanda yapılabilecek diğer çalışmalardan bahsedilmiştir. Vaka analizleri sonucu elde edilen değerler tekrar vurgulanmıştır.

Çalışma kapsamında rüzgar ve çevresel etkileri değerlendirerek çözümlenen rota optimizasyonuyla havacılığın iklim üzerindeki olumsuz etkilerinin düşürüldüğü gösterilmiştir. İleride bu çalışmadan yola çıkılarak çalışılabilecek konulardan bahsedilmiştir.

1. INTRODUCTION

The global aviation industry has been growing considerably in recent years. In the European airspace, the number of flights has increased and there are over 30000 flights per day especially in recent years. By improving aviation industry, operating costs and environmental impact of aviation become critically important issues. As indicated in European Aviation Environmental Report 2019, 3% of global carbon emissions is caused by aviation [1]. Furthermore, the Covid-19 pandemic has triggered a financial catastrophe in the aviation industry in all around the world. Air traffic in the United States declined by 33.5 percent in 2020 as a result of the COVID-19 pandemic, resulting in 5.3 million fewer flights than in 2019. In 2020, the number of flights in Europe fell by 55.2%, resulting in 6.1 million fewer flights than in 2019 [2]. Because of the fact that fuel corresponds to up to one quarter of the cost and accounts for over 97% of airline CO2 emissions [2], the airliners give priority to reduce fuel consumption in terms of both financial and environmental issues. In order to achieve this goal, for not only cost savings but also decrease the reverse effect of the aviation to the environment, trajectory based operations (TBO) have a huge importance. Besides this, there are various of approaches for saving more fuel and pollution reductions such as designing the aircraft structures with respect to decrease drag, utilizing sustainable aviation fuel, and performance improvements. In the near future, by highly demand increase on aviation, it is anticipated that the use of biofuels at a certain rate will become mandatory amongst aviation stakeholders.

Trajectory optimization, which has been studied since 1960s, is a dynamic research field. The four-dimensional - space and time - optimization is the cornerstone of the TBO and flying through the generated optimum route is caused to reduce fuel consumption and time. Until now, there are numerous of approaches is used to solve this problem. Taking account into wind, by means of direction and magnitude, affects the precision of results. Models that include wind forecasts give more realistic results than non-including ones as in real flights headwinds and tailwinds are of utmost importance to calculate the speed of an aircraft. It is widely known that under the effect of headwind the aircraft's speed is increased, on the contrary, in case of tailwind aircraft's speed is decreased. Utilizing tailwind is beneficial, in the meaning of flying in lower speeds which is also directly related with the less fuel consumption and aircraft emissions, especially for cruise stage of flights.

The wind-weather optimized aircraft trajectory generation framework is illustrated in Figure 1.1.

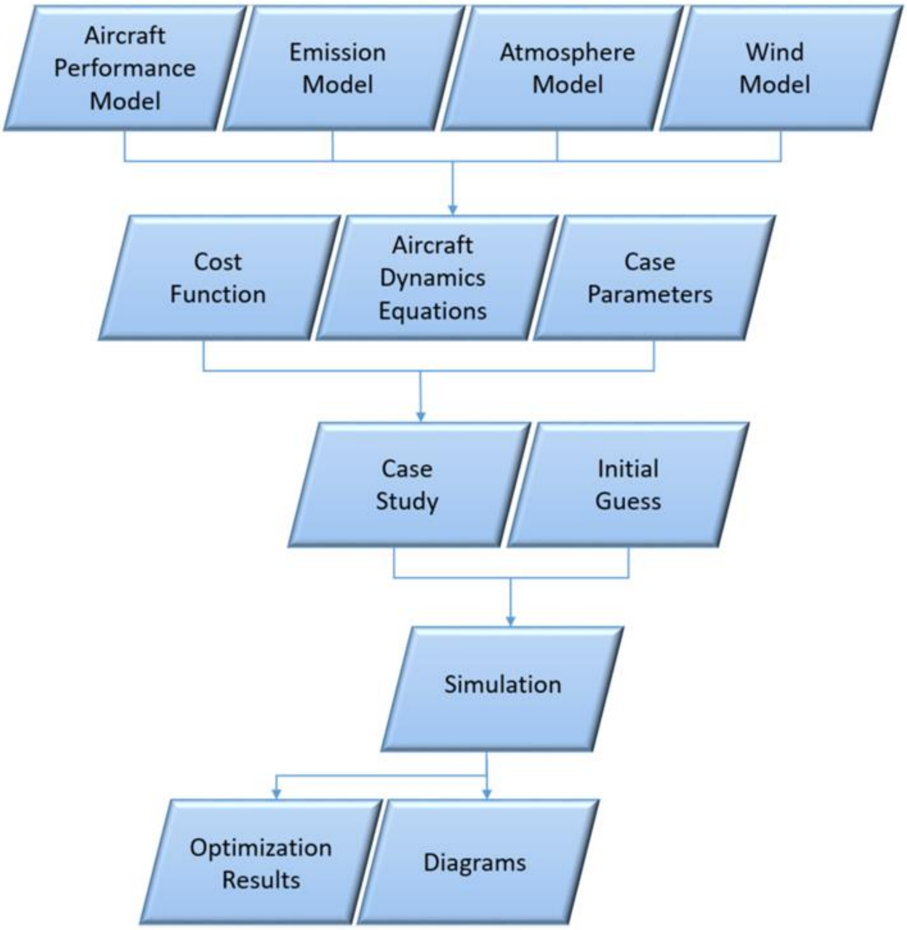

Figure 1.1: The wind-weather optimized aircraft trajectory optimization framework.

This master thesis tackles the aircraft trajectory optimization problem under wind effect by using optimal control techniques and evaluates the adverse impact of aviation in terms of aircraft emissions such as CO_2 and NOx. The presented model is constructed for cruise stage to find optimum trajectories with numerical simulations. The wind-optimized flight trajectories are considered to be a significant measure to reduce fuel consumption and flight duration. Optimized flight trajectories had obtained for 2D case (lateral) and 3D case (lateral and vertical). The parameters temperature, pressure as well as air density assumed as standard atmosphere values. Performance model used is based on BADA 4. In comparison, BADA 4 gives more realistic outcomes, which are evaluated in the conclusion part, than BADA 3. In order to get wind-optimized trajectories many numerical experiments carried out by using GEKKO Python Optimization package which is used to model such large type scale optimization gives accurate results to solve optimal control problems. The following framework related trajectory optimization sequences are given in order to make this thesis subject clear. The algorithm has been constructed to analyze the aviation effect on the environment via released aircraft emissions such as nitrogen oxides and carbon dioxide by using real air traffic data.

1.1 Scope of Thesis

This master thesis purpose is to present the efficiency of wind-optimized trajectories to reduce aircraft pollutants such as nitrogen oxide and carbon dioxide. The scope of the thesis are listed below:

- To introduce the first implementation of the wind optimal trajectory optimization problem to the Turkish Airspace.
- Real-time air traffic data and wind data used to generate optimum trajectories by considering minimum time, fuel consumption and aircraft emissions.
- To interpret the simulation results on the basis of environmental concerns.

1.2 Literature Review

In open literature, in order to find wind-optimal aircraft trajectories Girarget et al. in [3] proposed a wind-optimal path-planning algorithm that is based on Ordered Upwind Method in two-dimensional space. The Ordered Upwind Method is beneficial to avoid iterations as it is based on an analytical solution. Spherical coordinates were used within this study to get more precise results for long haul flights than to find the shortest distance between two points. In [4], flight planning with respect to minimum time is presented in free route airspace in a two dimensional space. The solution approach based on a shortest path algorithm. On the other hand, to simplify the problem, only flight time was taken into account in objective function and the problem is solved for 2D space. Legrand et al. in [5] addressed a new robust trajectory planning approach against unpredictability in wind. The efficient wind optimal algorithm is based on two stages that comprise first to get wind optimal trajectories by using classical Bellman algorithm and then clustering algorithm that based on a new mathematical distance calculation is used. In [6], Sridhar et al. assess the benefits of taking account of wind to find optimal routes. Cruise phase is considered for the reason that it is the major part of consumed fuel in entire flight. Simulations have done for trans-Atlantic routes because of the fact that it is the busiest oceanic airspace in the world. By flying wind-optimal route, fuel burn saving is estimated roughly 2.42% which means 760 kg for a wide body aircraft. In [7], investigation of improvement of European flight efficiency by wind optimized routing presented. DLR's trajectory optimization tool used to solve the optimization problem. In the result, the proposed model increased overall efficiency for not only fuel consumption but also flight time by 4.3% for a day which has advantageous in terms of tailwinds. The significant of the study is the first use of O.T.T.O. within DLR's simulation environment for calculating optimal routes with rising flight efficiency. Arribas et al. in [8] has introduced the effectiveness of robust optimal control to solve aircraft trajectory planning problems for cruise stage. The aim of the study [8] is while reducing the effect of meteorological uncertainty, improving the predictability of aircraft trajectories efficiently. In [9] handled the multi-objective 4D aircraft trajectory optimization based air traffic management (ATM). Fuel flow, time and distance take into account to construct a multi-criteria cost function. The main purpose of the study is generating routes that passes through the aviation obstacles. Zillies et al. in [9] proposed an algorithm that employs Lagrangian relaxation to generate optimal solutions comprises of new flight plans for scheduled traffic to follow, while conserving defined safety distance all the time. This study tested successfully for up to 200 flights, however, in order to improve the study and to apply realistic traffic scenarios, diverse atmospheric conditions should be taken into account. Soler et al. in [10], was tackled four dimensional flight planning problems with multiphase optimal control framework for commercial aircrafts. They claimed that an efficient flight planning should not only reduce fuel but also time by choosing effective trajectories and altitudes, speed and amount of fuel. The solution approach consists of at first multiphase optimal control problem is converted to optimal control problem. Then, optimal control problem is adapted by using a Hermite-Simpson collocation method. Consequently, a nonlinear programming problem (NLP) in hand is solved by using the IPOPT solver. This study indicates that inaccurate optimal initial mass estimation cause an increment by 0.75% in fuel consumption.

Nowadays, a number of investigation related to climate optimized flight trajectories has increased. The work in [11] added environmental impact in terms of climate and weather situation into the four-dimensional aircraft trajectory optimization problem in presence of winds. This study conducted by assumption of free flight conditions and constant Mach number, solely cruise trajectories were investigated. This study shown that 2D optimized flight trajectories can be able to reduce average temperature response (ATR) roughly 15% and in 3D case this percentage was increased to 20-35% higher. Soler et al. in [12] was handled the design of flight trajectory problem, by using mixed-integer optimal control approach which provides a solution for both discrete and continuous components, for climb and descent phase. Persistent contrail formation and CO2 emissions were taken into account besides fuel consumption and travel time in the cost function. It is widely known that contrails have critical effect on climate change as close as other air pollutants. In [13], Sridhar et al. was studied trajectory optimization of an aircraft under wind effect and persistent contrail avoidance. As aforementioned before in [12], condensation trails have negative impact on climate. The cost function consists of time, fuel, and passing through penalty areas. In this study, a 2% increase in overall fuel usage can cut contrail travel times by more than six times while optimizing altitude. Because of the complexity of computations, many studies including this thesis conducted the research for a specific aircraft and use one-day flight data. Lührs et al. in [14] proposed a network model, which aims climate impact reduction and cost increase, for climate and weather optimized routes in the North Atlantic flight corridor by using optimal control techniques. For simplicity, the results were evaluated for a single weather condition and 40 routes with a given specific altitude. As a result, it has been observed that around 24% to 32% of climate impact savings are achieved with 1% to 8% cost penalties. However, air traffic restrictions were not included in the study, these results were based on the assumption of free flight condition. In [15], the same subject which is 3D aircraft trajectory design for Trans-Atlantic flights, has been studied but this time by taking carbon dioxide and condensation traces into account by using dynamic programming. This study had shown that the total absolute global temperature change potential (AGTP) reduced to 38% with additional 3.1% fuel burn and flight time for eastbound flights and this AGTP ratio reduced to 20% with slightly more fuel consumption and less flight time for westbound flights. These results demonstrated that eastbound flights provide more environmental benefits and less additional fuel consumption than westbound flights because flying against to the strong headwinds causes more additional fuel use and emissions [15]. In [16], aircraft trajectories were evaluated in terms of multi-criteria environmental -noise and climate- impact of an aircraft's emissions. The significant result of this study is, while climate impact quantitatively measured between roughly 10% and 25% with supplemental fuel, the noise could not be measured quantitatively.

1.3 Thesis Structure

In the first chapter, the general overview on the topic and the problem are introduced. The purpose and contribution of the thesis are also given in this part. The literature review correlated to the optimum trajectory generation with various approaches are summarized.

In chapter two, the definition of the optimization problem and the mathematical model are given. The background information in which optimal control theory and its solution techniques are briefly explained to understand the problem clearly. Finally, the solution technique is defined and explained.

In chapter three, generation of the wind-weather optimized trajectory is described with all details. First of all, in order to simply the problem the assumptions are explained. The aircraft dynamics is defined by giving the aircraft's equations of motion for lateral (2D) and both lateral and vertical cases (3D). Besides that, the aircraft performance model defined by means of performance parameters for BADA 3 and BADA 4 are introduced. Lastly, wind model and emission models are presented. In wind model part, data preprocessing and multiple regression analysis are explained and visualized.

In chapter four, numerical simulations are conducted. The simulation results are evaluated for case studies.

In chapter five, to sum up, the study briefly explained again. The impact of the wind-weather optimized trajectory generation is discussed. Consequently, the future works which possibly can be done and its solution methods are introduced.

2. PROBLEM FORMULATION

In this section, the mathematical background of trajectory optimization problem is introduced with solving methods. In order to generate wind-weather optimized trajectories, optimal control techniques were used in this study. The aim is to minimize the cost functional, which comprises fuel consumption, travel time, and aircraft emission, subjected to physical limitations that call dynamic and algebraic constraints. Consequently, the objective and constraint models are presented within this chapter.

2.1 General Form of Optimal Control Problem

The general optimal control problem formulation, which aims to minimize objective, has given in Bolza form:

$$\min\ J\big(t, \boldsymbol{x}(t), \boldsymbol{u}(t)\big) = \Phi\big(t_0, t_f, \boldsymbol{x}_0, \boldsymbol{x}_f, \boldsymbol{u}_0\big) + \int_{t_0}^{t_f} L\big(\boldsymbol{x}(t), \boldsymbol{u}(t)\big)dt \qquad (2.1)$$

Subjected to:

$$\dot{\boldsymbol{x}}(t) = f(\boldsymbol{x}(t), \boldsymbol{u}(t), \boldsymbol{p}, t);\ t \in \big[t_0, t_f\big] \qquad (2.2)$$

$$x(t_0) \in \big[x_{min,0}; x_{max,0}\big] \qquad (2.3)$$

$$x\big(t_f\big) \in \big[x_{min,f}; x_{max,f}\big] \qquad (2.4)$$

$$x(t) \in [x_{min}; x_{max}] \qquad (2.5)$$

$$u(t) \in [u_{min}; u_{max}] \qquad (2.6)$$

$$p(t) \in [p_{min}; p_{max}] \qquad (2.7)$$

where $\boldsymbol{x}(t)$ describes the state variables, $\boldsymbol{u}(t)$ describes the control variables, $\boldsymbol{p}(t)$ is the path vector, t_0 is the initial time and t_f is the final time, i.e. the initial and final positions are $\boldsymbol{x}_0 = \boldsymbol{x}(t_0)$ and $\boldsymbol{x}_f = \boldsymbol{x}\big(t_f\big)$ respectively.

2.2 Optimal Control Solution Techniques

To find analytical solution of optimal control problem even for a simple model is a challenging task because of its extremely nonlinearity condition [10]. For this reason, numerical methods are used to solve continuous time optimal control problem which are indicated below:

- Dynamic programming methods
- Indirect methods
- Direct methods

2.2.1 Dynamic programming methods

The optimality criteria is based on the Hamilton-Jacobi-Bellman partial differential equation in continuous time [17]. The principle of using DP is to divide problem into subproblems primarily. Then, the solution is obtained by solving these subproblems recursively.

The main drawback of DP is , because of the "curse of dimensionality," a term developed by Bellman to explain the problem caused by the exponential increase in the size of the state space, the dynamic programming method is suitable for solving discontinuous system problems.

The inherent characteristic of aircraft trajectory optimization problem, DP is not suitable method for solution because the aspects of nonlinearity and continuity.

2.2.2 Indirect methods

Indirect methods use variational calculus and Pontryagin's maximum principle, in order to obtain optimality conditions. The calculus of variations, unlike ordinary calculus (where the goal is to find points that optimize a function), is concerned with finding functions that optimize a function of a function (also known as functional optimization) [18].

The working principle of the method is to discretize the boundary value problem after optimization. The indirect methods are insufficient to solve engineering problems. The issue is that adjoin equations are frequently devoid of physical significance, making them impossible to solve even with physically reasonable initial approximations. This is due to the fact that the Hamiltonian generates a boundary value problem with a high numerical precision, which may result in trajectories that surpass the computer's numerical range [19].

2.2.3 Direct methods

Contrary to indirect methods, the principle of direct methods follow first discretize and then optimize approach which means infinite dimensional problem is converted to finite dimensional problem and then this reduced problem is solved by using optimization methods [19]. A common strategy is to transform the infinite dimensional problem into a nonlinear programming problem (NLP) that could be solved by using mathematical programming methods [20].

The three main direct methods are direct single shooting method, direct multiple shooting method and direct collocation method. Especially, direct collocation methods are widely used in order to solve trajectory optimization problems in open literature.

The optimal control problems with initial guesses can be easily converted into an NLP problem with direct single shooting method. By comparison, this method is critically affected by initial guess perturbations [27].

The direct multiple shooting method may increase the size of the problem by increasing the number of constraints and variables. When inequality constraints are included, there is the added drawback of having to specify the sequence of unconstrained and restricted arcs ahead of time [27].

Among direct methods, the direct collocation method which consist of Hermite-Legendre-Gauss-Lobatto approach is the best method to solve aircraft trajectory optimization problem. A convenient interpolating function is called interpolant is chosen that passes through the state values and sustains the derivatives of state at the nodes that span one time period. Then, the interpolant is assessed at collocation points between nodes. Collocation methods are identified by the interpolant, by the nodes and collocation points [10]. Another member of direct collocation methods is pseudospectral approach. The convergence rate of pseudospectral approach is exponential which means converges swiftly.

2.3 Constraints

There are several constraints on state and control variables. The states can be represented as $x = [x, y, h, v, \psi, m]^T$ and the controllers can be represented as $u = [\gamma, \phi, \delta]^T$. The general notation of the path constraints can be written as follows:

$$\left.\begin{array}{r} x_{min} \leq x \leq x_{max} \\ y_{min} \leq y \leq y_{max} \\ h_{min} \leq h \leq h_{max} \\ v_{min} \leq v \leq v_{max} \\ \psi_{min} \leq \psi \leq \psi_{max} \\ m_{min} \leq m \leq m_{max} \end{array}\right\} \quad (2.8)$$

and

$$\left.\begin{array}{r} \gamma_{min} \leq \gamma \leq \gamma_{max} \\ \phi_{min} \leq \phi \leq \phi_{max} \\ \delta_{min} \leq \delta \leq \delta_{max} \end{array}\right\} \quad (2.9)$$

2.4 Optimization Problem

The optimization problem is constructed with respect to minimize flight time, fuel consumption and NO_x emissions. The parameters temperature, pressure and air density are calculated based on the ISA (International Standard Atmosphere) assumption. Aircraft performance model used is based on BADA. In order to find the optimum path with respect to wind vector for cruising aircraft in a three dimensional space is interested within this study. In the scope of the study, optimal control techniques are used to model for three-dimensional flight trajectories. A non-linear optimal control problem with path constraints are solved to find wind-optimized trajectories [13]. Wind-optimized flight trajectories and numerical simulations are programmed in Python with GEKKO Python Optimization package. The following optimal control problem is constructed to obtain an optimized trajectory in a wind field:

$$\min\ \left(x(t_f) - x_d\right)^2 + \left(y(t_f) - y_d\right)^2 + \int_0^{t_f} \left(c_1 f + c_2 + c_3 \theta^{-0.425} e^{0.2M^2} f\right) dt \quad (2.10)$$

subjected to:

$$aircraft\ dynamics\ (3.14)\ -\ (3.19)$$

$$T = T_{SL} - \beta h \quad (2.11)$$

$$p = p_{SL} \left(T / T_{SL}\right)^{\frac{g}{\beta R}} \quad (2.12)$$

$$\rho = \frac{p}{RT} \quad (2.13)$$

$$C_L = \frac{2mg_0}{\rho S v^2 cos\phi} \tag{2.14}$$

$$C_0 = g(d_{1:5}, M) \tag{2.15}$$

$$C_2 = g(d_{6:10}, M) \tag{2.16}$$

$$C_6 = g(d_{11:15}, M) \tag{2.17}$$

$$C_D = A.\left[C_0 + C_2 {C_L}^2 + C_6 {C_L}^6\right] \tag{2.18}$$

$$C_T = g(a_{1:36}, \delta_T, M) \tag{2.19}$$

$$Thr = \delta_p . W_{m_{ref}} . C_T \tag{2.20}$$

$$C_F = g(f_{1:25}, C_T, M) \tag{2.21}$$

where $d_{1:15}, a_{1:36}, f_{1:25}$ are obtained from BADA. A is the scaling factor depends on the aircraft type. The c_1, c_2, and c_3 are coefficients that determine the weight of fuel consumption, flight time and nitrogen oxide production over the objective function, respectively. When the study [30] in which the emission model is obtained is examined, it can be deduced that nitrogen oxides are produced proportionally with the term $\theta^{-0.425} e^{0.2M^2}$ in the ISA case, therefore, thanks to this term added to the objective function, nitrogen oxides, which have a significant effect on climate change, production is also aimed to be reduced. The optimization problem will aim to produce the best solution by considering both cases.

2.5 Solving Optimal Control Problem

The optimal control problem described by the cost functional, the constraints and the controllers are solved by using the GEKKO that is a Python based optimal control package. GEKKO is a package that includes the ability to run model predictive control, dynamic parameter estimation, real-time optimization, and parameter update for dynamic models on real-time applications, as well as an algebraic modelling language (AML) for posing optimization problems in simple object-oriented equation-based models to interface with powerful built-in optimization solvers [33]. The nonlinear programming (NLP) problem has solved utilizing GEKKO solves the NLP problem with respect to the principle that first discretize the continuous optimal control problem and then solve as in direct approach.

3. WIND-WEATHER OPTIMIZED TRAJECTORY GENERATION

In this section, 3-DoF point-mass model aircraft on the basis of BADA 4 and the wind model is presented in order to construct the optimization problem. In Figure 3.1, the flowchart of trajectory generation is presented.

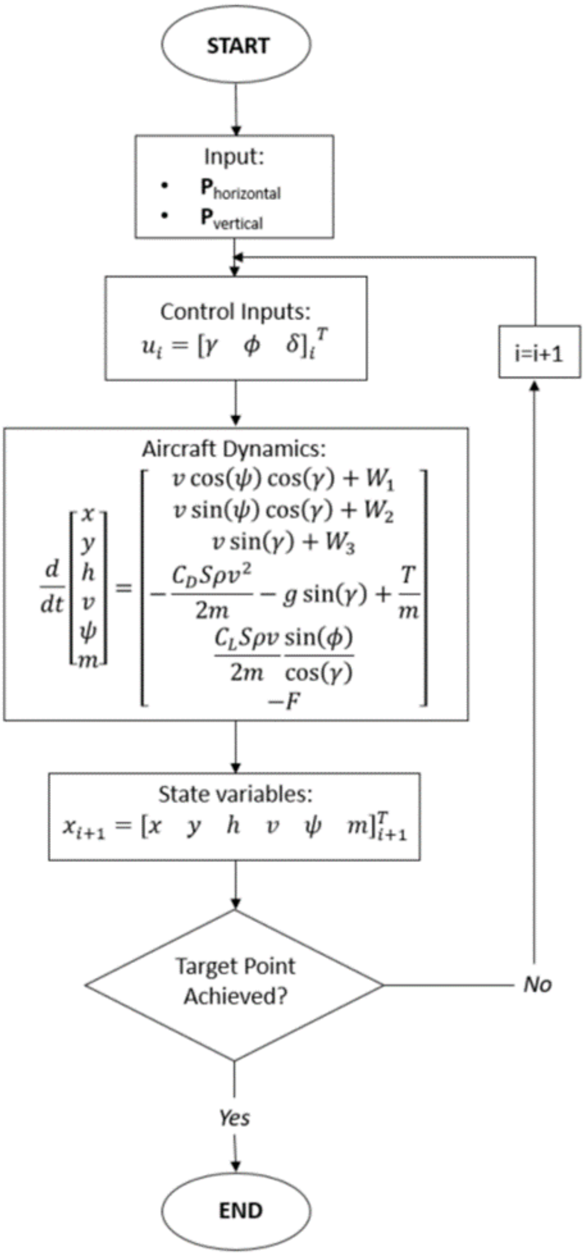

Figure 3.1: The flowchart of wind-weather optimized trajectory generation.

Primarily, assumptions which simplify the problem in order to make computationally solvable by the computer in a logical time and atmosphere model are introduced. Then, aircraft dynamic and performance model are explained in details. The section is concluded by describing the wind model and the emission model that are used for environmental impact assessment.

3.1 Assumptions

The aircraft point-mass model (PMM), which only take into account translational dynamics not rotational dynamics, is used within the numerical simulations. To simplify the model, rotational dynamics that occurs because of the torques and moments is ignored.

By flat and non-rotating Earth assumption, the Earth's rotation and nearly ellipsoid shape, which make problem mathematically complex, are neglected.

International Standard Atmosphere (ISA) Model is used to determine atmospheric conditions such as air density, pressure and temperature based on BADA Family 4.

3.2 Atmosphere Model

Based on the International Standard Atmosphere (ISA) model, this section is presented formulas for atmospheric properties such as pressure, temperature, air density, and speed of sound as a function of altitude. In order to calculate fuel consumption of an aircraft, the international standard atmosphere model which assumes that the air is devoid of dust, moisture and water vapor is used. Also, the air is assumed to be at rest, in other words no winds and turbulence [21]. The equations in atmosphere model are based on BADA 4.

3.2.1 Determination of air pressure and temperature

The Earth's atmosphere is divided to two layers, troposphere and stratosphere, by tropopause which has a constant altitude. The geopotential pressure altitude is $H_{p,trop} = 11{,}000\ [m]$ in tropopause.

From the mean sea level (MSL) ($H_p = 0\ [m]$), to 11,000 meters corresponds to troposphere ($H_p \leq 11{,}000\ [m]$). The temperature and air pressure equations for troposphere indicated in equations 3.1 and 3.2 below. In troposphere, as to go higher altitudes above sea level, the temperature decreases linearly but the air pressure decreases exponentially.

Temperature:

$$T_<(H_p) = T_0 + \beta_{T,<} \cdot H_{p<} \tag{3.1}$$

Air Pressure:

$$P_<(H_p) = P_0 \left(\frac{T_<}{T_0}\right)^{-\left(\frac{g_0}{\beta_{T,<} R}\right)} \tag{3.2}$$

From 11,000 meters to 25,000 meters corresponds to stratosphere ($H_p > 11{,}000$ [m]). In stratosphere, while air pressure decreases exponentially, temperature is constant. The temperature and air pressure equations for stratosphere seen in equations 3.3 and 3.4 below.

Temperature:

$$T_>(H_p) = T_{trop} \tag{3.3}$$

Air Pressure:

$$P_>(H_p) = P_{trop} \exp\left[-\frac{g_0}{R \cdot T_{ISA,trop}}\left(H_{p,>} - H_{p,trop}\right)\right] \tag{3.4}$$

3.2.2 Determination of air density

The density of air, ρ [kg/m^3] could calculated at altitude as:

$$\rho = \frac{P}{RT} \tag{3.5}$$

There is an inverse proportion between altitude and air density. While altitude is increasing, air density decreases. In this notation, p represents the pressure and T is the temperature.

3.2.3 Determination of Mach number

The speed of sound is defined as the rate at which pressure waves flow throughout a fluid, as expressed by the equation 3.6 [23].

$$a = \sqrt{\kappa RT} \tag{3.6}$$

The speed of sound changes with respect to temperature. The temperature decrement at higher altitudes causes Mach number changes as it directly related with the speed of sound. The Mach number could be found with respect to the true airspeed V_{TAS} [m/s] and the temperature, for a particular altitude by using the equation 3.7.

$$M = \frac{v}{\sqrt{\kappa R T}} \tag{3.7}$$

3.2.4 The standard atmosphere model parameters

The standard atmosphere model parameters are given based on BADA 4. The physical parameters with respect to mean sea level (MSL) which means the geopotential pressure altitude (H_p) is equals to zero. The parameters based on BADA 4 are demonstrated their values with units in Table 3.1.

Table 3.1: The standard atmosphere model parameters based on BADA 4.

Parameter	Description	Value	Unit
T_0	Standard Atmospheric Temperature at MSL	288.15	[K]
P_0	Standard Atmospheric Pressure at MSL	101325	[Pa]
$\beta_{T,<}$	Lapse Rate	-0.0065	[K/m]
g_0	Gravitational Acceleration	9.80665	[m/s^2]
R	Real Gas Constant for Air	287.05287	[m^2/(K.s^2)]
κ	Adiabatic Index of Air	1.4	[-]

3.3 Aircraft Dynamics

The general representation of the aircraft's time-invariant dynamics is as follows [24]:

$$\dot{x}(t) = f\big(x(t), u(t)\big); \quad x(t_0) = x_0 \tag{3.8}$$

where $x: X \subseteq \mathbb{R}^a$ and $u: U \subseteq \mathbb{R}^b$ such that $a, b \in \mathbb{N}$. At initial condition $t_0 = 0$, the state of the aircraft is $x_0 \in X$ and $u(t)$ is the control input. The aircraft dynamic models for both two- and three- dimensional case, are described by assuming that the point-mass aircraft motion over the flat and non-rotating Earth.

3.3.1 2D aircraft model

The equations of motion (EoM) of a 2-DoF aircraft dynamic model defined as follows:

$$\dot{x} = v\cos(\psi) + W_1 \tag{3.9}$$

$$\dot{y} = v\sin(\psi) + W_2 \tag{3.10}$$

$$\dot{v} = -\frac{C_D S\rho v^2}{2m} + \frac{Thr}{m} \tag{3.11}$$

$$\dot{\psi} = \frac{C_L S\rho v}{2m}\sin(\phi) \tag{3.12}$$

$$\dot{m} = -F \tag{3.13}$$

The two-dimensional model consists of five state variables (x, y, v, ψ, m) and two control inputs (ϕ, γ). The states includes, longitude and latitude (x and y), the true airspeed (v), the heading angle (ψ) and mass (m). The controllers are the bank angle (ϕ). The wind speed is modeled as $W = [W_1, W_2]$, W_1 is the east-west component and W_2 is the north-south component of the wind vector.

3.3.2 3D aircraft model

The equations of motion (EoM) of a 3-DoF aircraft dynamic model defined as follows:

$$\dot{x} = v\cos(\psi)\cos(\gamma) + W_1 \tag{3.14}$$

$$\dot{y} = v\sin(\psi)\cos(\gamma) + W_2 \tag{3.15}$$

$$\dot{h} = v\sin(\gamma) + W_3 \tag{3.16}$$

$$\dot{v} = -\frac{C_D S\rho v^2}{2m} - g\sin(\gamma) + \frac{Thr}{m} \tag{3.17}$$

$$\dot{\psi} = \frac{C_L S\rho v}{2m}\frac{\sin(\phi)}{\cos(\gamma)} \tag{3.18}$$

$$\dot{m} = -F \tag{3.19}$$

The nonlinear dynamical model consists of six state variables and three control inputs. The state variables are longitude and latitude (x and y), altitude (h), the true airspeed (v), the heading angle (ψ) and the aircraft mass (m); that is, $x(t) = \big(x(t), y(t), h(t), v(t), \psi(t), m(t)\big)$. The control inputs the flight path angle (γ), the bank angle (ϕ), and the thrust lever position (δ); that is, $u(t) = \big(\gamma(t), \phi(t), \delta(t)\big)$. The wind speed $W = [W_1, W_2, W_3]$ is taken into account as a disturbance (i.e. W_1, W_2, W_3 are components of the wind vector on the spherical coordinates). The other parameters in the set of equations above are aerodynamic force components lift coefficient (C_L) and drag coefficient (C_D), the surface are of wing (S), air density (ρ) and fuel consumption (F).

3.4 Aircraft Performance Model

The cornerstone to plan the effective real-life air traffic operations is the reliable trajectory prediction. The simulation environment has to be capable of preplanning of the air activities as realistically as possible. The trajectory predictor tools are based on Aircraft Performance Models (APM). Therefore, EUROCONTROL, with aircraft manufacturer's contribution, has developed BADA which contains specifications of theoretical model and particular datasets for precisely simulating the behavior of an aircraft throughout the flight envelope and for all flight phases.

The comprehensive and accurate aircraft performance and operation models have a tremendous impact on aviation concerns such as minimization of fuel consumption, reduction of air pollutants and air traffic density. Currently, there are two existing BADA version which are BADA 3 and BADA 4.

BADA 3 is the first developed model which aimed to meet requirements of aircraft performance model over a nominal part of flight envelope [25]. These requirements are related to the modeled aircraft's performance accuracy, the operational flight envelope coverage, the represented flight phases, and the type of operation that APM supports [26]. The model specifications of the entire aircraft types is available in BADA 3. The primary flaw of BADA 3 cannot give an efficient model for the entire aircraft operational envelope. In order to model and simulate advanced systems for future concept of ATM, BADA 4 was presented. However, BADA 4 only contains eighty percent of aircraft types.

As illustrated in Figure 3.1 [26], BADA is structured into two parts which are Aircraft Performance Model (APM) and Airline Procedure Model (ARPM). Aircraft Characteristics can be defined with coefficients which are used by these two models for a specific type of aircraft.

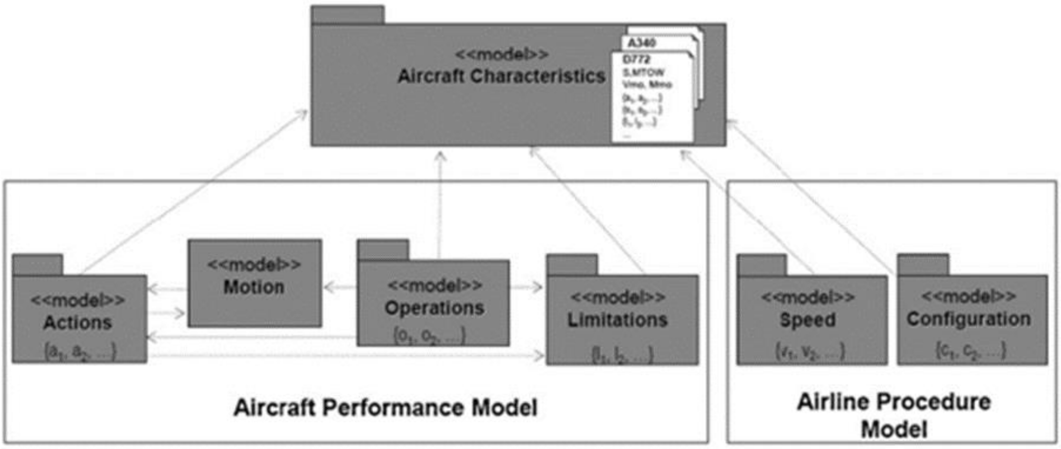

Figure 2.2: The structure of BADA model.

Aircraft Performance Model (APM) has four sub-models that are actions, motion, operations and limitations. Action model provides to compute aerodynamic actions (lift and drag forces), propulsive actions (engine thrust and fuel consumption) and gravitational actions (weight force). Motion and operations model identify the aircraft equations of motion and the ways of operation of the aircraft, respectively. Limitations model defines limits and restricts behavior of the aircraft to ensure safe and realistic operation.

Airline Procedure Model (ARPM), which provides information on nominal aircraft operations for each flight phases, comprises speed model and configuration model. It is generally known as, the manner, an aircraft is operated changes greatly depending on specific airspace procedures and operating rules of prominent airlines in the area. Therefore, the BADA standard airline procedure model's generating speed schedules may vary from a certain geographical region or a aerospace's specific aircraft operation [26].

The aerodynamic coefficients, engine thrust, and fuel consumption equations are compared with respect to BADA Family 3 and BADA Family 4 within the following section. All the numerical simulations were performed utilizing Boeing B738 aircraft performance model.

3.4.1 BADA 3 aircraft performance parameters

3.4.1.1 Aerodynamics

The lift coefficient (C_L) and drag coefficient (C_D) are shown as follows:

$$C_L = \frac{2 \cdot m \cdot g_0}{\rho \cdot V^2 \cdot S \cdot cos\phi} \tag{3.20}$$

$$C_D = C_{D_0} + C_{D_2} C_L^2 \tag{3.21}$$

where m is the mass of the aircraft [kg], g_0 is the gravitational acceleration [m/s^2], ρ is the air density [kg/m^3], V is the true airspeed [m/s], S is the wing reference area [m^2] and ϕ is the bank angle [rad].

In equation of 3.21, C_{D_0} and C_{D_2} vary according to the climb, cruise, approach, takeoff and landing flight phases.

3.4.1.2 Engine thrust

The coefficients for three thrust levels which are maximum climb and takeoff, maximum cruise and descent is provided by BADA 3. The units of results are given in Newtons (N). Cruising flight phase for jet engine type is examined within the scope of this master thesis, thus, only the equations for cruise phase associated to climb phase are presented. The equations of descent ignored. The expressions for turboprop and piston engine type are also available in BADA 3 document [22].

- **Maximum climb thrust**

$$(Thr_{max})_{climb} = C_{Tc,1} \cdot \left(1 - \frac{H_p}{C_{Tc,2}} + C_{Tc,3} \cdot H_p^2\right) \tag{3.22}$$

- **Maximum cruise thrust**

$$(Thr_{max})_{cruise} = C_{T_{cr}} \cdot (Thr_{max})_{climb} \tag{3.23}$$

In equation 3.22, H_p denotes to geopotential altitude and $C_{Tc,1}, C_{Tc,2}, C_{Tc,3}$ are the thrust coefficients provided by BADA 3. Although, by the definition thrust is equal to drag in cruise flight phase, the maximum cruise thrust is limited as indicated in equation 3.23.

3.4.1.3 Fuel consumption

The fuel consumption is highly dependent to two dominant parameters, the thrust specific fuel consumption (η) and the fuel flow (f_{nom}). For turbojet and turboprop engine types have the same equations.

- **The thrust specific fuel consumption**

  For the jet engine type, the thrust specific fuel consumption expression is as follows:

$$\eta = C_{f1} \cdot \left(1 + \frac{V}{C_{f1}}\right) \quad (3.24)$$

  The unit of the thrust specific fuel consumption (η) is [kg/min.kN].

- **The nominal fuel flow**

  For the jet engine type, the nominal fuel flow expression is as follows:

$$f_{nom} = \eta \cdot T(H_p) \quad (3.25)$$

  The unit of the nominal fuel flow (f_{nom}) is [kg/min]. By the definition, consumption of the mass of fuel in a second gives the nominal fuel flow. Thus, the nominal fuel flow is determined by the thrust (T).

- **The cruise fuel flow**

  For the jet engine type, the cruise fuel flow expression is as follows:

$$f_{cr} = C_{fcr} \cdot \eta \cdot T(H_p) \quad (3.26)$$

  The unit of the cruise fuel flow (f_{cr}) is [kg/min]. The cruise fuel flow is calculated utilizing the thrust specific fuel consumption (η), the thrust (T) and a cruise fuel flow correction factor (C_{fcr}). The cruise fuel flow correction factor (C_{fcr}) has been determined to increase the efficiency of cruising aircraft.

According to BADA 3, the fuel consumption equation for cruise phase can be written as below:

$$\dot{m} = -C_{fcr} \cdot \eta \cdot T_{max}(H_p) \cdot \delta_P \quad (3.27)$$

3.4.2 BADA 4 aircraft performance parameters

3.4.2.1 Aerodynamics

The lift coefficient (C_L) is shown in the following equation:

$$C_L = \frac{2 \cdot m \cdot g_0}{\delta_P \cdot P_0 \cdot \kappa \cdot M^2 \cdot S \cdot cos\phi} \quad (3.28)$$

where m is the mass of the aircraft [kg], g_0 is the gravitational acceleration [m/s^2], δ_P is the pressure ratio [-], P_0 is the standard atmospheric pressure at MSL [Pa], M is the Mach number [-], κ is the adiabatic index of air [-], S is the wing reference area [m^2] and ϕ is the bank angle [rad].

The drag increase caused by the deployment of high-lift devices and landing gear is accounted for by aerodynamic drag [26]. The configurations of high-lift devices and landing gear are categorized as clean or non-clean. In case of expansion on the high-lift devices and landing gear, non-clean configuration is used, otherwise clean configuration is used.

- **Clean configuration**

  In clean configuration, the Mach number is less than or equal to M_{max}, the drag coefficient can be modelled as:

  $$C_D = A \cdot [C_0 + (C_2 C_L^2) + (C_6 C_L^6)] \tag{3.29}$$

  subjected to:

  $$C_0 = g(d_{1:5}, M) \tag{3.30}$$

  $$C_2 = g(d_{6:10}, M) \tag{3.31}$$

  $$C_6 = g(d_{11:15}, M) \tag{3.32}$$

  where A is scaling factor [-] depends on the aircraft type, C_L is the lift coefficient [-], M is the Mach number [-], $d_{1:15}$ are clean drag coefficients [-] are obtained from the clean drag polar model (DPM).

- **Non-clean configuration**

  In non-clean configuration, the Mach number is less than or equal to M_{max}, the drag coefficient can be modelled as:

  $$C_D = d_{1_{\delta_{HL},\delta_{LG}}} + d_{2_{\delta_{HL},\delta_{LG}}} C_L + d_{3_{\delta_{HL},\delta_{LG}}} C_L^2 \tag{3.33}$$

  where C_L is the lift coefficient [-], δ_{HL} is the position of the high-lift devices [-], δ_{LG} is the position of the landing gear [-], $d_{1:3_{\delta_{HL},\delta_{LG}}}$ are non-clean drag coefficients [-] are obtained from the aerodynamic forces and configurations model (AFCM).

In this study, by the reason that cruise phase is investigated, the calculations had done utilizing clean configuration.

3.4.2.2 Engine thrust

The equation for engine thrust has indicated below:

$$T = \delta_P \cdot W_{m_{ref}} \cdot C_T \tag{3.34}$$

where δ is the pressure ratio [-], $W_{m_{ref}}$ is the reference weight force at m_{ref} [N], in addition m_{ref} is the reference mass [kg] obtained from the propulsive forces model (PFM) and C_T is the thrust coefficient [-] which varies with respect to type of engine.

The thrust coefficient, C_T, is calculated for idle rating or non-idle rating. The difference between idle rating or non-idle rating can be explained as while non-idle rating equation is used in case of maximum climb and cruise, idle rating is used for descent.

- **Idle rating**

  The idle rating model has shown below for turbofan engine types as:

$$C_T = g\left(t_{i_{1:12}}, \delta_P, M\right) \tag{3.35}$$

  where δ_P is the pressure ratio [-], M is the Mach number [-], $t_{i_{1:12}}$ are idle rating thrust coefficients [-] obtained from the turbofan Model (TFM).

- **Non-idle Rating**

  The non-idle rating model for maximum cruise (MCRZ) has shown below for turbofan engine types as:

$$C_T = g(a_{1:36}, \delta_T, M) \tag{3.36}$$

  where δ_T is the throttle parameter [-], M is the Mach number [-], $a_{1:36}$ are non-idle rating thrust coefficients [-] obtained from the turbofan Model (TFM).

Because of the reason that this study had done for cruise phase, the non-idle rating model is used in calculations.

3.4.2.3 Fuel consumption

The model of fuel consumption is shown below:

$$F = \delta_P \cdot \theta^{\frac{1}{2}} \cdot W_{m_{ref}} \cdot a_0 \cdot L_{HV}^{-1} \cdot C_F \tag{3.37}$$

where δ_P is the pressure ratio [-], θ is the temperature ratio [-], $W_{m_{ref}}$ is the reference weight force at m_{ref} [N], in addition m_{ref} is the reference mass [kg] retrieved from the propulsive forces model (PFM), a_0 is the speed of sound at mean sea level (MSL) in standard atmosphere [m/s], L_{HV} is the fuel lower heating value [m^2/s^2] retrieved from the propulsive forces model (PFM), C_F is the fuel coefficient [-].

The calculation of C_F varies for idle and non-idle ratings,

$$C_F = \begin{cases} C_{F_{idle}}, & for\ idle\ rating \\ \max\left(C_{F_{gen}}, C_{F_{idle}}\right), & non-idle\ rating \end{cases} \tag{3.38}$$

- **Idle rating**

$$C_{F_{idle}} = g\left(f_{i_{1:9}}, \delta_P, M, \theta\right) \tag{3.39}$$

where δ_P is the pressure ratio [-], θ is the temperature ratio [-], M is the Mach number [-], $f_{i_{1:9}}$ are idle rating fuel coefficients [-] from the turbofan Model (TFM).

- **Non-idle rating**

$$C_{F_{gen}} = g(f_{1:25}, C_T, M) \tag{3.40}$$

where C_T is the thrust coefficient [-], M is the Mach number [-], $f_{1:25}$ are non-idle rating fuel coefficients [-] from the turbofan Model (TFM).

Non-idle rating model is used in numerical simulations.

3.5 Wind Model

The wind velocity is made up of two parts: a deterministic component that represents the ATC's meteorological predictions, and a stochastic component that indicates the uncertainty in those predictions [27]. The deterministic component of wind is taken into account within this study.

The meteorological predictions are retrieved from the Global Forecast System (GFS). The Global Forecast System (GFS) is a weather forecast model has developed by the National Centers for Environmental Prediction (NCEP). The analysis and forecast grids for the NCEP operational Global Forecast System are 0.25°×0.25° global latitude longitude grids. Grids have analysis and forecast time steps every 3 hours from 0 to 240, and every 12 hours from 240 to 384. Daily model forecast runs take place at 00, 06, 12, and 18 UTC [28]. The wind considered as stationary that means changing over time does not take into account. The wind field of European airspace for a day illustrated in Figure 3.3.

Wind forecasts retrieved from GRIB files as west, north and vertical components of the wind velocity vector for each node of the grid. GRIB data is provided with respect to spherical coordinates: longitude, latitude and altitude. The general representation of the wind vector is $W = (W_1, W_2, W_3)$. In order to adopt the wind data into to model, an analytical expression is required. Thus, the multivariate polynomial regression has been applied within this model.

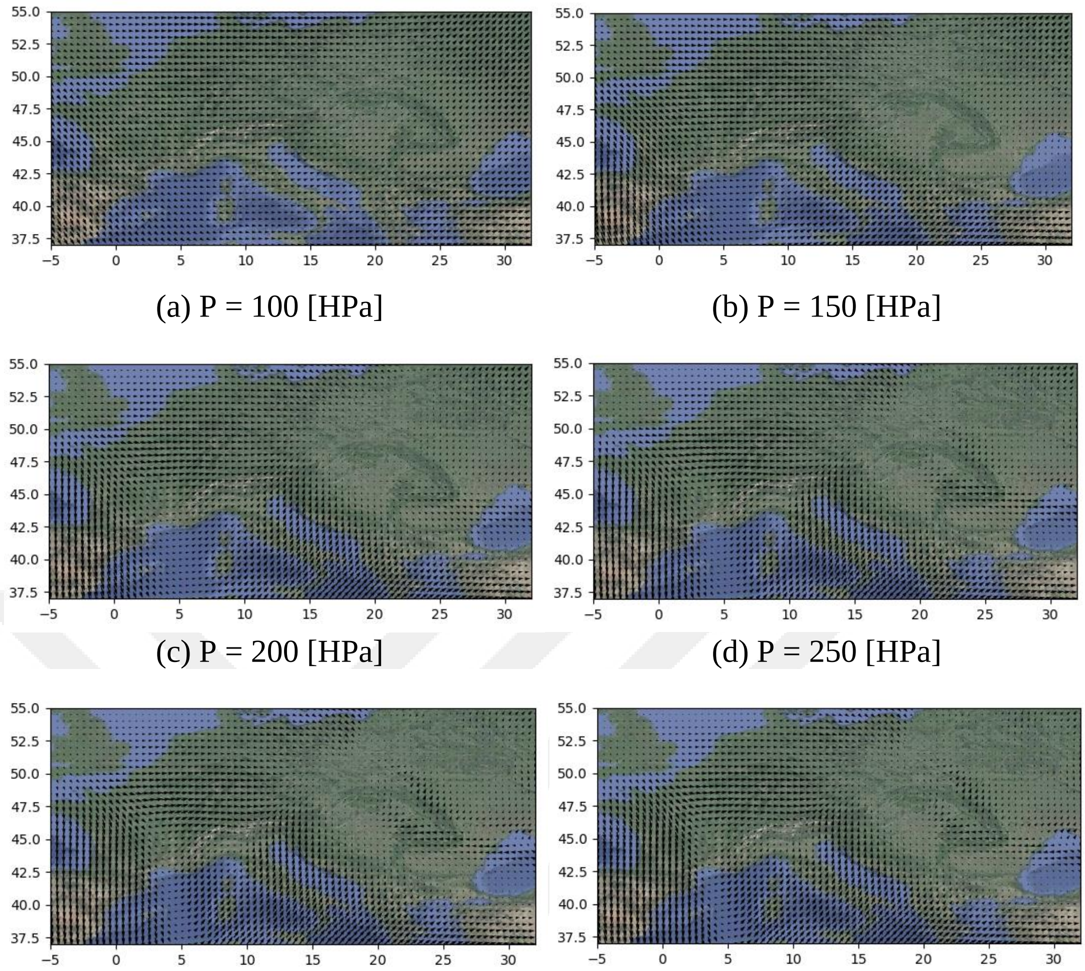

(a) P = 100 [HPa] (b) P = 150 [HPa]

(c) P = 200 [HPa] (d) P = 250 [HPa]

(d) P = 300 [HPa] (e) P = 350 [HPa]

Figure 3.3: The wind field of European Airspace for a different barometric altitudes.

The general representation of polynomial regression for n independent variables is shown below [12]:

$$Y = \beta_0 + \beta_1 X_1 + \beta_2 X_2 + \beta_3 X_3 + \cdots + \beta_n X_n + \varepsilon \quad (3.41)$$

where $\{\beta_0, \beta_1, \beta_2, \beta_3, \dots, \beta_n\}$ are the coefficients of regression and ε is the error component. In case of, there is no linear association among all of the variables, polynomial regression is essentially required.

The coefficients of the multivariate polynomial regression equation was estimated utilizing least-square method. Therefore, the polynomial regression equation becomes [12],

$$\hat{Y} = \hat{\beta}_0 + \hat{\beta}_1 X_1 + \hat{\beta}_2 X_2 + \hat{\beta}_3 X_3 + \cdots + \hat{\beta}_n X_n \quad (3.42)$$

where $\{\hat{\beta}_0, \hat{\beta}_1, \hat{\beta}_2, \hat{\beta}_3, \dots, \hat{\beta}_n\}$ are the estimated coefficients or in other terms least-squares estimates and $\hat{Y}$ is the value which has been predicted. The least-squares method explains that the best-fitting curve is represented by the fact that the sum of squares of all deviations (S) from supplied values must be the minimum, i.e.:

$$S = \sum_{j=1}^{n} \left(Y_j - \hat{Y}_j\right)^2 \tag{3.43}$$

Regression analysis, fairly simple analytical functions for a given set of tabular data, but at the cost of less precision in fitting the data than cubic spline interpolation, making it a feasible task to include wind data in the optimal control problem [27]. For this reason, regression analysis with polynomial functions is used in this thesis.

3.5.1 Data preprocessing

The wind speed measurement is affected by several factors such as contrails, unexpected fall in wind speed etc. Thus, the GRIB files have non-uniform order in terms of the magnitude of wind speed. The sudden enormous increment or decrement in wind speed which causes error could be observed in GRIB datas. Data can be changed after it has been compiled to remove or lessen any volatility or other types of noise which is called data smoothing. Data smoothing is a powerful technique to get rid of this sudden changes and to continue with the suitable set of data.

One of the most common method for data approximation is interpolation. In order to reduce the average of the squares of the errors, the data approximation was performed by using the cubic spline approach within this study. Error calculations were made using the mean square error method between real and adjusted data.

The wind forecast data set smoothed separately for the meridional and zonal wind components. Data smoothing for selected three days are shown, specific to Turkish airspace, in Figures 3.4, 3.5 and 3.6 below.

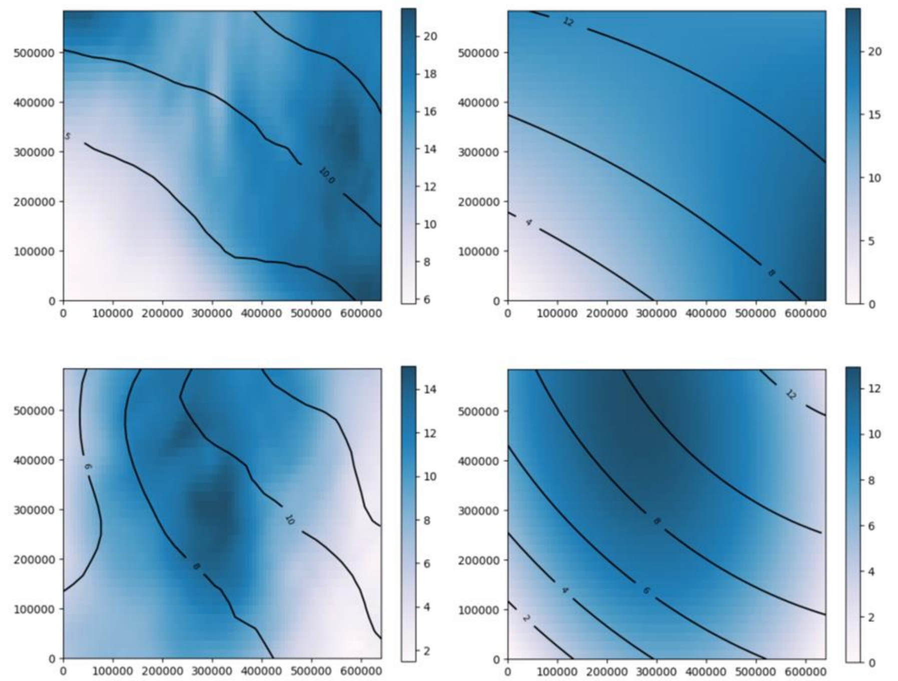

Figure 3.3: The data smoothing of horizontal wind components (in m/s) on October 1, 2018. The upper plots are for x component of wind (real wind data has shown on the left and smoothed data has shown on the right) and the lower plots are for y components of wind (real wind data has shown on the left and smoothed data has shown on the right).

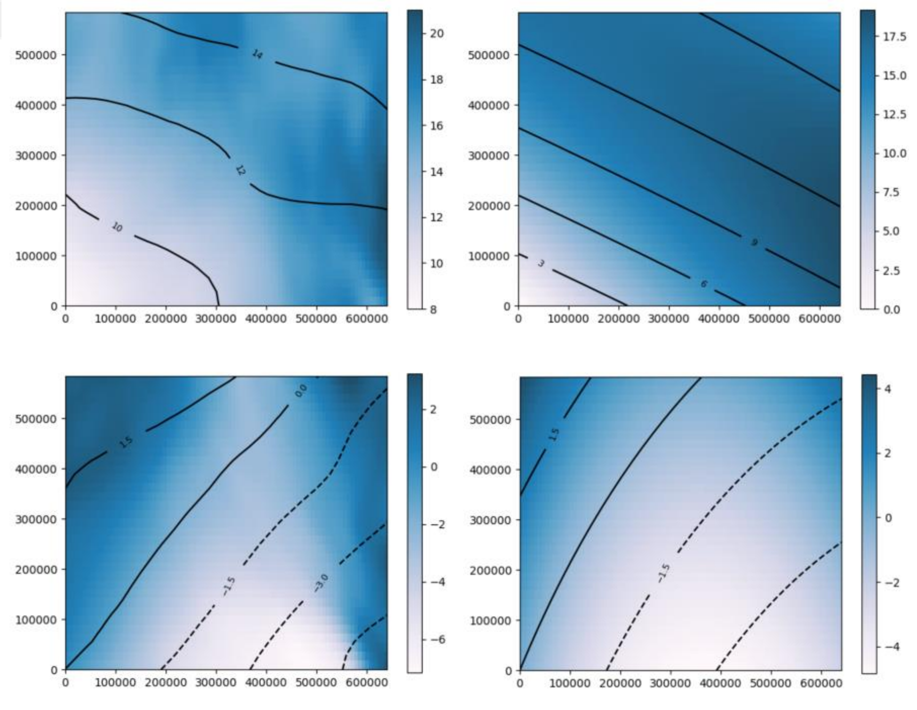

Figure 3.5: The data smoothing of horizontal wind components (in m/s) on October 5, 2018. The upper plots are for x component of wind (real wind data has shown on the left and smoothed data has shown on the right) and the lower plots are for y components.

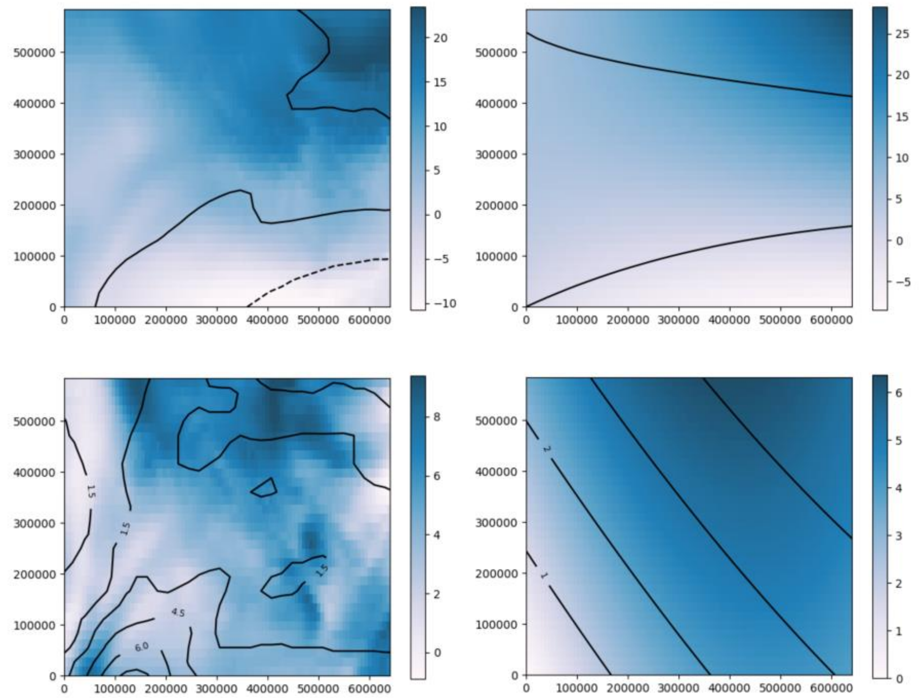

Figure 3.6: The data smoothing of horizontal wind components (in m/s) on October 7, 2018. The upper plots are for x component of wind (real wind data has shown on the left and smoothed data has shown on the right) and the lower plots are for y components.

3.5.2 Multiple regression analysis

Multivariate polynomial regression is a form of a polynomial regression where more than one variable is considered. The polynomial regression formulation is given above (see equation 3.41). The velocity of a wind vector, W, is presented in a n grid points in this dissertation's scenario, and to estimate the value of the wind velocity vector at each point, three dimensional multivariate polynomial regression should be used. The equation (3.41), within this situation, becomes as shown in below [27]:

$$Y(x_e, y_e, z_e) = \beta_{000} + \beta_{100}x_e + \beta_{010}y_e + \beta_{001}z_e + \beta_{200}x_e^2 + \beta_{110}x_e y_e + \beta_{020}y_e^2 + \beta_{101}x_e z_e + \beta_{011}y_e z_e + \beta_{002}z_e^2 + \cdots + \beta_{00n}z_e^n + \varepsilon \quad (3.44)$$

where $Y(x_e, y_e, z_e): \mathbb{R}^3 \to \mathbb{R}, (x_e, y_e, z_e) \in \mathbb{R}^3$ and $\beta_{000}, \beta_{100}, \beta_{010}, \dots, \beta_{00n}$ are the coefficients.

According to GRIB data, the vertical component of the wind is not considered (i.e. $W_3 \approx 0$) and the zonal and meridional components of the wind which are W_x and W_y are independent from each other. Therefore, the analysis of multivariate regression had been conducted for both horizontal components separately.

The analytical expression for east-west component of the wind velocity can be calculated as [12]:

$$W_x = \beta_{000}^1 + \beta_{100}^1 x_e + \beta_{010}^1 y_e + \beta_{001}^1 z_e + \beta_{200}^1 x_e^2 + \beta_{110}^1 x_e y_e + \beta_{020}^1 y_e^2 + \beta_{101}^1 x_e z_e + \beta_{011}^1 y_e z_e + \beta_{002}^1 z_e^2 + \cdots + \beta_{00n}^1 z_e^n + \varepsilon_1 \quad (3.45)$$

The analytical expression for north-south component of the wind velocity can be calculated as [12]:

$$W_y = \beta_{000}^2 + \beta_{100}^2 x_e + \beta_{010}^2 y_e + \beta_{001}^2 z_e + \beta_{200}^2 x_e^2 + \beta_{110}^2 x_e y_e + \beta_{020}^2 y_e^2 + \beta_{101}^2 x_e z_e + \beta_{011}^2 y_e z_e + \beta_{002}^2 z_e^2 + \cdots + \beta_{00n}^2 z_e^n + \varepsilon_2 \quad (3.46)$$

In these equations, $\beta_{000}^1, \ldots, \beta_{00n}^1$ and $\beta_{000}^2, \ldots, \beta_{00n}^2$ are the coefficients of regression and according to this study, x_e and y_e correspond to longitude and latitude, z_e corresponds to altitude.

According to the wind forecast data set, the analytical functions are calculated separately for the meridional and zonal components of the wind. In the figures below, specific to Turkish airspace, the regression analyses for selected three days are shown. The analytical functions (see equations 3.45 and 3.46) are indicated with surface and wind forecast tabular data for each grid point is indicated with blue dots.

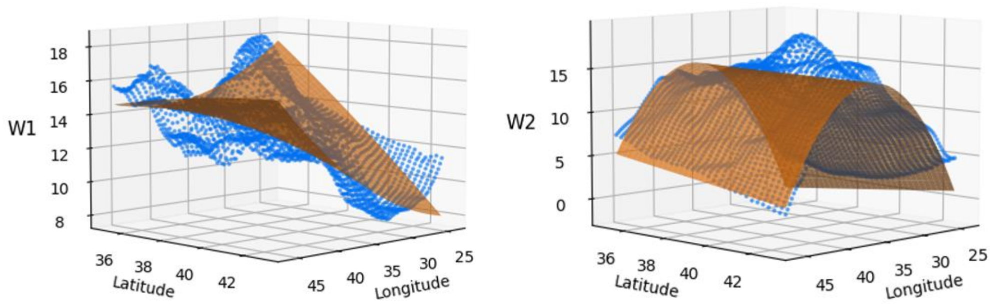

Figure 3.7: The regression analyses of horizontal wind components (in m/s) on October 1, 2018 at 150 [HPa] barometric altitude.

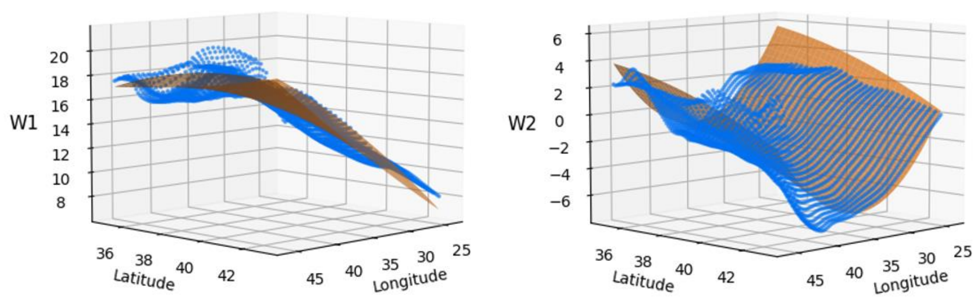

Figure 3.8: The regression analyses of horizontal wind components (in m/s) on October 5, 2018 at 100 [HPa] barometric altitude.

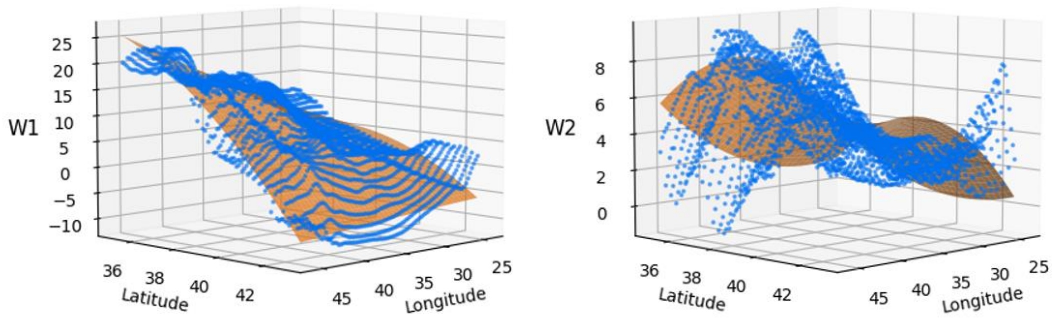

Figure 3.9: The regression analyses of horizontal wind components (in m/s) on October 7, 2018 at 350 [HPa] barometric altitude.

3.6 Emission Model

The global emission monitoring techniques are becoming more crucial in supporting political decision-making, with the growing public interest in problems about aviation's environmental impact [31]. The cornerstone of political decision-making process is to provide reliable operational data from airliners. However, the emission information for a specific engine type is available only for ground level. In ICAO Engine Exhaust Emission Databank, the change in Mach number, aircraft mass and altitude, which are necessary in order to investigate cruise stage, are not taken into account in data. Until now, the error margins has been decreased below %30 and the datum has been improved for more aircraft and engine types.

The fuel burn estimations based on BADA fuel flows are highly close to real ones. Similarly, the same fact may be drawn for the proportionate pollutants produced by fuel combustion, such as H_20, NO_x, and CO_2. NO_x results are consistent with past domain expert project estimates and are based on BM2-EEC modified, a modification of the commonly recognized and accepted BM2 approach [31]. The emission indices for NO_x, HC, and CO during the LTO (Landing and Takeoff) cycle which is base for the fuel burn calculations below 3000 ft, are presented in the ICAO Engine Exhaust Data Bank. Besides that, above 3000 ft, the fuel burn calculation is based on BADA which is also used in this study. The diagram below depicts a simplified representation of the various methodologies used by AEM3 to obtain the most realistic fuel burn estimates for each phases of the flight profile [31].

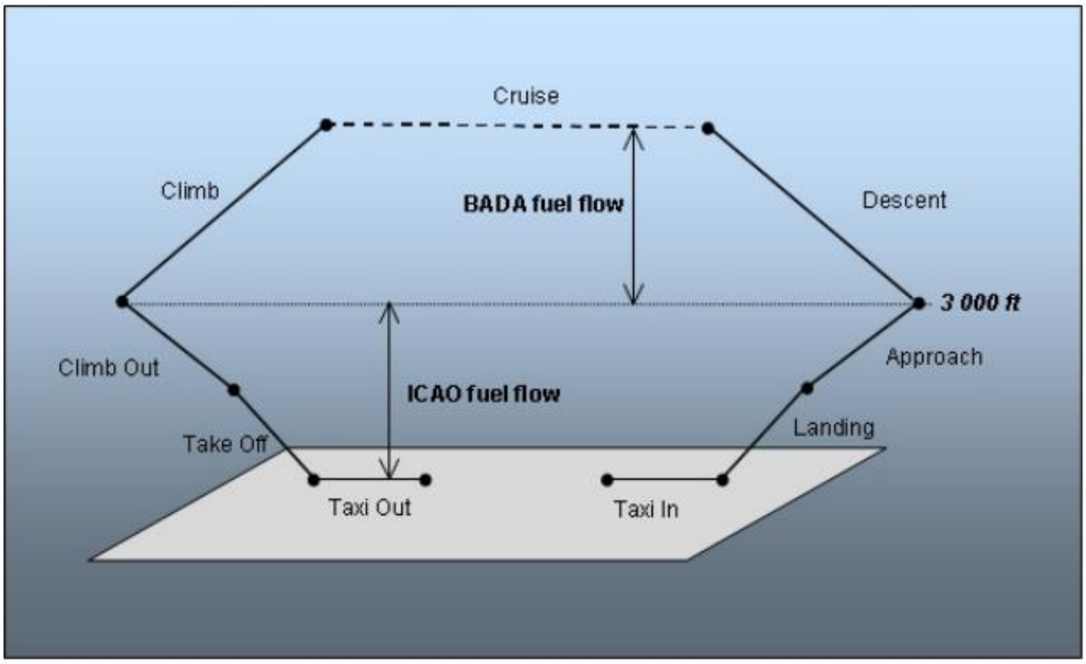

Figure 3.10: Fuel calculation cycle of the AEM3.

Air pollutants such as NO_x and CO_2, are attracted attention because of their significant economic cost on anthropogenic climate change. According to the findings, cruise phase emissions are responsible for 90% of global impacts per unit of fuel burned, while air quality impacts account for 64% of all damages. Moreover, nitrogen oxides (NO_x), carbon dioxide (CO_2), and contrails account for 97 percent of the entire impact [32]. Therefore, while computing optimized trajectories, to include the cost of emissions in the objective function has a huge importance to reduce adverse impact of aviation in terms of gaseous emissions. In order to find the relation between fuel burn and pollutants, it is necessary to measure of fuel consumption. Estimating air pollutants can be done by two methods. CO_2, H_2O and SO_2 are all exactly proportional to the amount of fuel used, the calculation have done by using the coefficients that have the value of 3.149 kg / kg Fuel, 1.230 kg / kg Fuel and 0.00084 kg / kg Fuel respectively. Other way for NO_x, HC and CO is using Boeing Method 2 for over 3000 ft Non-LTO phases and ICAO Engine Exhaust Emissions Data Bank for below 3000 ft LTO flight phases. The table below visualizes the information aforementioned before:

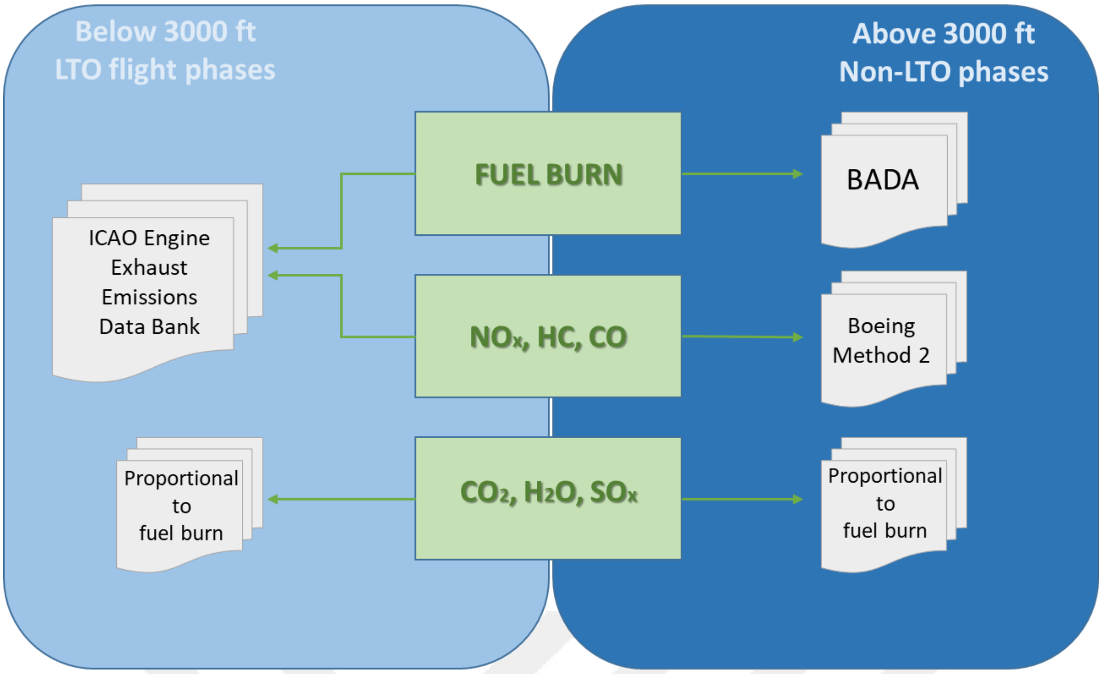

Figure 3.11: Fuel burn and emission calculations for AEM3.

The emission model has constructed depends on the ICAO Engine Exhaust Data Bank [29] and Boeing Method 2 [30]. The aircraft emissions could be envisaged by Fuel Flow Method 2 (or Boeing Method 2). The emissions indices correction equation of nitrogen oxide (NO_x) on the ground demonstrated below [30]:

$$EINOx_{Alt} = EINOx_{Sl} \left(\frac{\delta_{amb}^{1.02}}{\theta_{amb}^{3.3}} \right)^{y} \tag{3.47}$$

where $EINOx_{Sl}$ is emission indices of NO_x at sea level, y is the engine/combustor unique which is empirically derived by the manufacturers and the value of y is between 0.2 and 0.5, the ambient density ratio that is $\delta_{amb} = P_{amb}/14.696$ and the ambient temperature ratio that is $\theta_{amb} = T_{amb}/518.67$.

Using the Boeing Method 2, these emission indices are adapted to higher altitudes. The engine fuel flow rate as a correction factor is calculated by the equation indicated below [30]:

$$W_{f_{SL}} = W_{f_{Alt}} \frac{\theta_{amb}^{3.8}}{\delta_{amb}} e^{0.2M^2} \tag{3.48}$$

where θ_{amb} is the ambient temperature ratio, δ_{amb} is the ambient pressure ratio and M is the Mach number.

As presented in the study [31] and aforementioned before, the emission index of CO_2 is presented as a constant coefficient (3.149 kg / kg Fuel), which is independent from the altitude.

Using this model, the released emissions for a defined trajectory can be calculated for both NO_x and CO_2.

4. SIMULATION AND RESULTS

In this chapter, firstly, simulation results are shown according to BADA 4. Then, the wind field over the route is investigated and illustrated. In the end, the numerical simulations are discussed with respect to fuel burn, travel time and NO_x and CO_2 emissions costs.

An B737-800 BADA 3.9 aircraft model was considered within numerical simulations. The various aerodynamic configurations are available in BADA.

4.1 Case Study 1: The Investigation of Turkish Airspace Specific to Istanbul to Ankara Flights

4.1.1 Problem setup

In this case study, trajectory optimization problem has been solved for cruising aircraft by considering realistic flight data from Istanbul Atatürk Airport to Ankara Esenboğa Airport in October 6, 2018. The B737-800 aircraft model and BADA performance limitations parameters are used in the numerical simulations.

The problem is build as a multi-objective optimization problem. The aim of the problem is to determine the least amount of fuel, NO_x emission and minimum time to complete the cruise phase of route while taking into account the actual factors that affect a commercial flight such as wind.

4.1.2 Wind data

The wind tabular data of October 6, 2018 in the Turkish airspace region have been examined i.e. $x_e \in [24°, 46°]$ and $y_e \in [35°, 43°]$. The multivariate polynomial regression has been applied to derive a meaningful analytical function from the wind forecasts that obtained from the Global Forecast System (GFS).

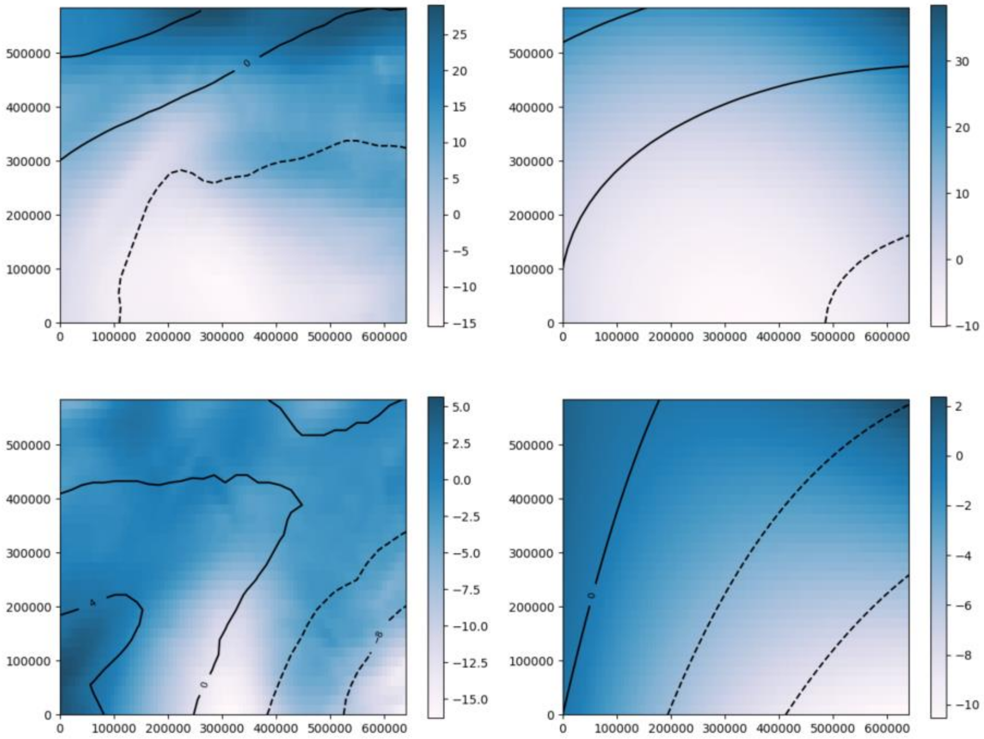

Figure 4.1: The data smoothing of meridional and zonal wind components (in m/s) at 300 [HPa] barometric altitude. The upper plots are for x component of wind (real wind data has shown on the left and smoothed data has shown on the right) and the lower plots are for y components.

The difference between real wind data and wind data produced by analytical functions yields 0.50 for W_x and 0.44 for W_y utilizing mean squared error method.

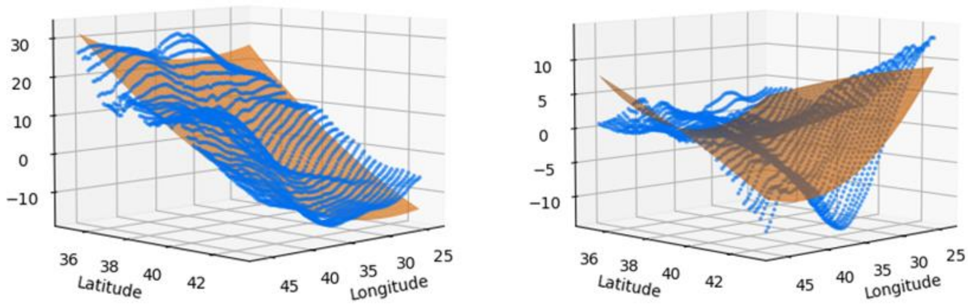

Figure 4.2: The magnitude of meridional (left) and zonal(right) wind components at 300 [HPa] indicates real wind forecasts (dots) and analytical functions (surfaces).

The polynomial functions of horizontal wind components, W_x and W_y, are calculated by using equations 3.45 and 3.46. In Figure 4.2, real wind data for each grid point at 300 [HPa] represented with blue dots and analytical functions represented with orange colored surfaces. In the graphs above, it is clearly seen that the actual data and the estimated data calculated using the wind model converge.

This study is conducted to find analytical wind equations for horizontal plane by using multivariate polynomial regression method. In order to get a single specific equation for meridional and zonal components of wind vector, fitting a specific polynomial for 3D space (longitude, latitude, altitude) has been given insufficient results. Therefore, analytical equations have been calculated according to flight time related csv. file for different flight levels in level flight.

4.1.3 Numerical results

The numerical simulation results for eighteen flights on October 6,2018 are shown in table below. In the following chapters, the results will be evaluated in terms of fuel consumption, travel time and environmental impact of air pollutants.

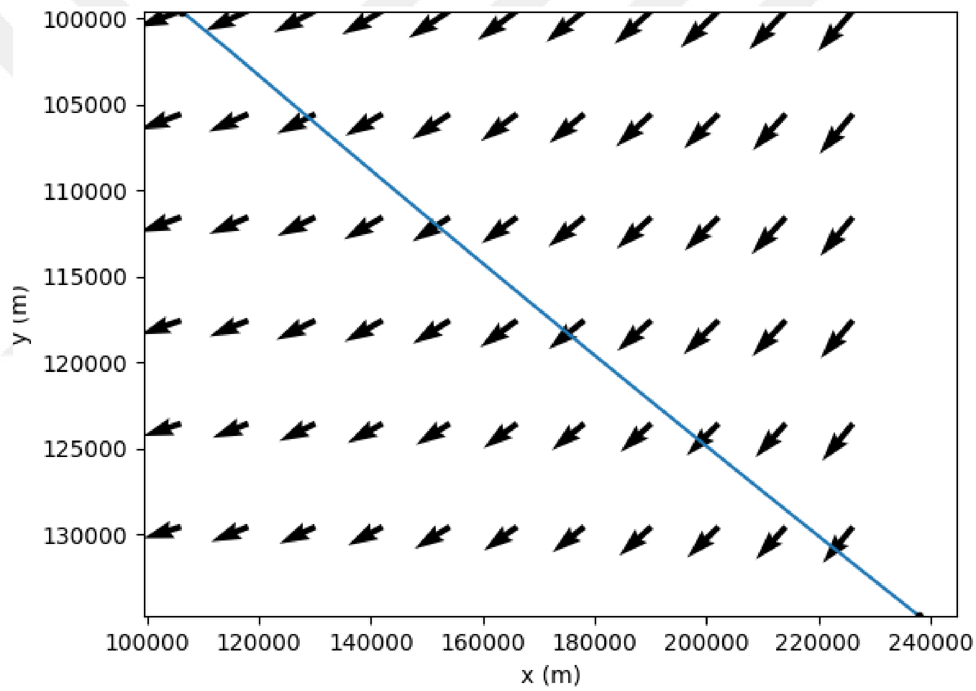

Figure 4.3: The wind-weather optimized trajectory for İstanbul – Ankara cruise flight.

Tablo 4 1: Optimization and flight plan results for Istanbul to Ankara flights on October 6, 2018.

FLIGHT NO	OPTIMIZATION RESULTS				FLIGHT PLAN RESULTS			
	NO_x EMISSION [kg]	CO_2 EMISSION [kg]	TIME [s]	FUEL [kg]	NO_x EMISSION [kg]	CO_2 EMISSION [kg]	TIME [s]	FUEL [kg]
1	3,892123363	1243,77283	491,9010021	394,973906	4,991911742	1516,753708	701	481,6620221
2	8,236918918	2782,585455	1131,541217	883,640983	10,17978057	3095,22685	1436	982,9237376
3	4,269934245	1598,030137	663,6334915	507,472257	5,656980251	1718,876605	795	545,848398
4	4,269934245	1598,030137	663,6334915	507,472257	5,947979573	1807,382175	836	573,9543268
5	5,938698806	2013,587107	800,5224243	639,436998	6,902101479	2098,230028	969	666,3162997
6	5,886999133	1999,601406	799,5689381	634,995683	7,01364677	2131,313322	986	676,8222679
7	5,886999133	1999,601406	799,5689381	634,995683	7,878440603	2394,452998	1108	760,3852011
8	5,983608908	2027,647266	807,8525719	643,901958	7,183971804	2183,134489	1010	693,2786564
9	6,009612067	2037,022935	811,5516739	646,879306	6,880631216	2091,707693	966	664,2450597
10	5,983608908	2027,647266	807,8525719	643,901958	7,183759475	2183,069309	1010	693,2579579
11	5,983608908	2027,647266	807,8525719	643,901958	7,204884775	2189,499412	1013	695,2999084
12	5,983608908	2027,647266	807,8525719	643,901958	7,205146802	2189,576175	1013	695,3242855
13	4,818385528	1693,290631	665,4549445	527,756651	5,564637996	1690,789169	782	536,9289201
14	5,557998839	2066,113167	849,047591	656,117233	7,321048529	2225,739548	1028	706,808367
15	6,185052868	2085,469767	824,7919184	662,264137	8,098180621	2461,323697	1139	781,6207358
16	6,016120667	2039,742688	821,246915	647,749803	6,89127605	2094,402991	970	665,1009817
17	6,185052868	2085,469767	824,7919184	662,264137	7,063144988	2146,371452	993	681,6041449
18	9,586305905	2890,798057	1156,193337	918,005099	9,783134461	2974,034008	1377	944,4376018

4.1.3.1 Fuel consumption

Fuel consumption was determined based on the differential equation 3.19. LTBA to LTAC flights in a day and their fuel consumptions for cruise flight phase had shown in table 2. According to the optimization results, approximately 638.87 [kg] fuel was consumed per flight while cruise stage and the total fuel consumption have been found as 11499.63 [kg]. As obtained from the results, fuel consumption has improved utilizing proposed mathematical model by 6.8% in comparison with real fuel consumption data. From the point of airliners, only for a single route, this rate is corresponds to approximately 812$ profit in terms of operational costs (Jet fuel price in Turkey was 0,858$ per liter for September 14, 2022).

4.1.3.2 Travel time

The results of numerical LTBA to LTAC flight simulations, travel times for each flight had shown in table 2. The average flight time for cruise flight phase, had been found roughly 808 [s] per flight. The average total improvement has found as %17.9 [s] by means of flight time.

4.1.3.3 NO_x and CO_2 emissions

The calculation of NO_x and CO_2 emissions are presented in Chapter 3.6. The amount of air pollutants had shown in table 2.

Optimization results indicate that the total amount of NO_x and CO_2 emissions for a day had found approximately 106.68 [kg] and 36243.71 [kg]. This means that, the average amount of emitted NO_x and CO_2 per flight is 5.93 [kg] and 2013.54 [kg] respectively. Thus, specific to LTBA (İstanbul Atatürk Airport) to LTAC (Ankara Esenboğa Airport) flights for a day, average total NO_x emissions have improved by 15.87% and CO_2 emissions have improved by 6.8%.

4.2 Case Study 2: The Investigation of European Airspace Specific to Paris to Frankfurt Flights

The multi-objective optimization problem has been solved for eleven flights from Paris Charles de Gaulle Airport (CGD) to Frankfurt Airport (FRA) with B737-800 aircraft, on a day (October 6, 2018) specific to cruise flight phase. In order to achieve more realistic model, wind vector has taken into account above this region.

4.2.2 Wind data

The wind tabular data of October 6, 2018 in the European airspace region has been examined i.e. $x_e \in [0°, 9°]$ and $y_e \in [50°, 45°]$. The multivariate polynomial regression has been applied to derive an analytical function from the wind forecasts that obtained from the Global Forecast System (GFS).

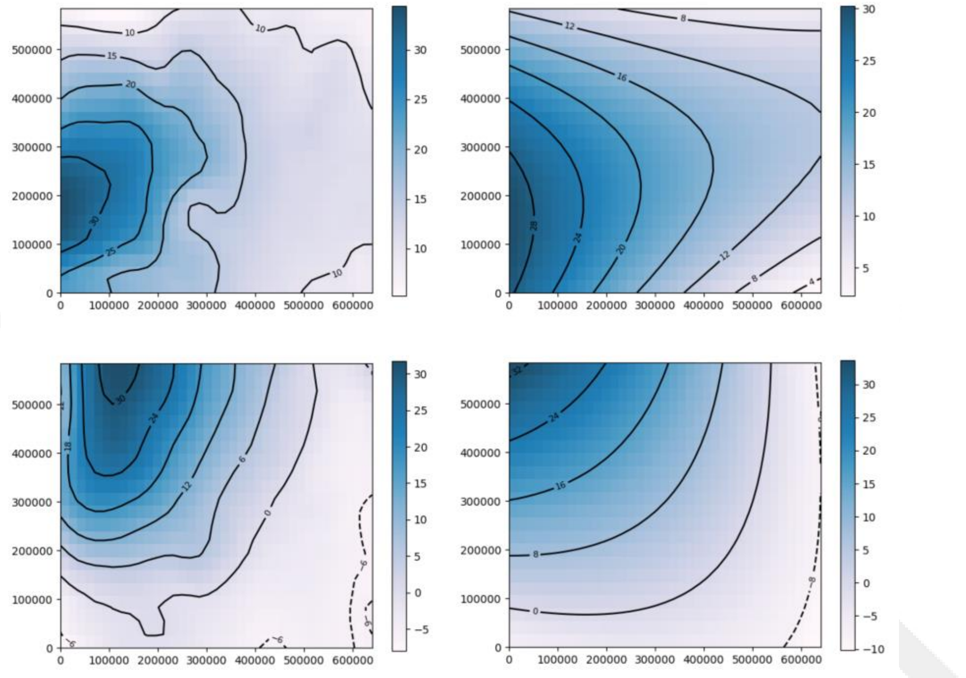

Figure 4.4: The data smoothing of meridional and zonal wind components (in m/s) at 300 [HPa] barometric altitude. The upper plots are for x component of wind (real wind data has shown on the left and smoothed data has shown on the right) and the lower plots are for y components.

The difference between real wind data and wind data produced by analytical functions yields 0.52 for W_x and 0.67 for W_y utilizing mean squared error method.

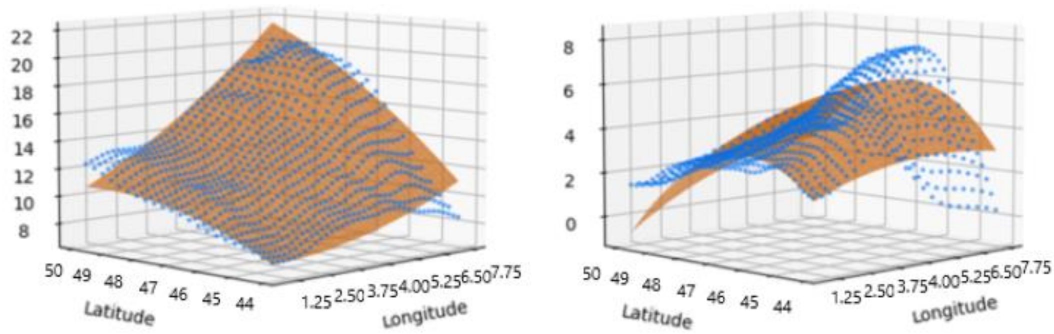

Figure 4.5: The magnitude of meridional and zonal wind components at 150 [HPa] shows real wind forecasts (blue dots) and analytical functions (surfaces).

The polynomial functions of horizontal wind components, W_x and W_y, are calculated utilizing equations 3.45 and 3.46. In figure 4.4, that actual wind data for each grid point are shown with blue dots and analytical functions are shown with orange surfaces. This study is conducted to find analytical wind equations for horizontal plane by using multivariate polynomial regression method. In order to get a single specific equation for meridional and zonal components of wind vector, fitting a specific polynomial for 3D space (longitude, latitude, altitude) has been given insufficient results. Therefore, analytical equations have been developed according to flight time related csv. file for different flight levels in level flight.

4.2.3 Numerical results

The simulation results are shown below for eleven flights on October 6,2018. According to fuel consumption, travel time and emissions, the results will be examined in the following sections.

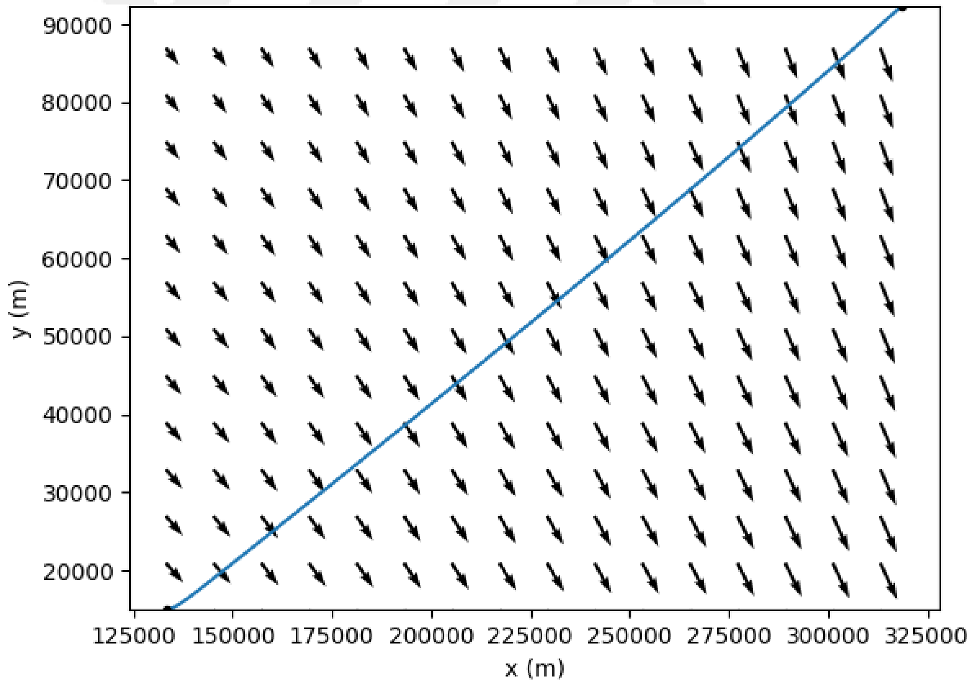

Figure 4.6: The wind-weather optimized trajectory for Paris – Frankfurt cruise flight.

Table 4.2: The optimization and flight plan results for Paris to Frankfurt flights on October 6,2018.

FLIGHT NO	OPTIMIZATION RESULTS				FLIGHT PLAN RESULTS			
	NO_x EMISSION [kg]	CO_2 EMISSION [kg]	TIME [s]	FUEL [kg]	NO_x EMISSION [kg]	CO_2 EMISSION [kg]	TIME [s]	FUEL [kg]
1	6,855527502	2067,671471	851,8952203	656,61209	7,930755567	2151,033165	841	683,0845237
2	7,339993101	2226,990453	919,3901095	707,205606	8,842535893	2379,611182	910	755,6720173
3	3,516357921	899,3255394	355,3758983	285,590835	3,795952967	1015,153587	386	322,3733206
4	9,191056075	2817,64543	1166,891185	894,774668	11,71767421	3089,331818	1147	981,0517047
5	9,248284532	3169,168293	1147,165549	1006,404666	16,09567736	3600,153598	1079	1143,268847
6	8,262947006	2532,338774	1052,486345	804,172364	9,97939582	2741,437346	1086	870,5739429
7	9,579284357	2956,221161	1232,545805	938,780934	11,1713651	3155,248215	1298	1001,98419
8	7,227285614	2201,33447	913,9354159	699,058263	11,87100819	2731,807067	834	867,5157406
9	8,064725543	2785,11569	1164,281755	884,444487	11,87357181	3270,827779	1296	1038,687767
10	6,85220163	2216,977024	820,181063	704,02573	11,57727457	2729,80437	863	866,8797617
11	8,95422818	2772,077781	1162,522373	880,304154	10,9363044	3071,002141	1268	975,2309117

4.2.3.1 Fuel consumption

All Paris Charles De Gaulle Airport to Frankfurt Airport flights in a day and their fuel consumptions during cruise phase has shown in table 3. The optimizations results demonstrate that roughly 769.22 [kg] fuel consumed per flight pursuant to cruise phase and totally 8461.37 [kg] of fuel used for all flights specific to the route. In comparison of flight plan data, fuel consumption is decreased around 9.9% by presented model. The rate of reduction of fuel consumption corresponds to 888$ profit in operational costs for Paris to Frankfurt cruise flights (Jet fuel price in France was 0,849$ per liter for September 14, 2022).

4.2.3.2 Travel time

As a result of numerical LFPG to EEDF flight simulations, it is obviously seen that the average cruise flight time has found as 981 [s]. This is also corresponds to %1.6 [s] decrement in terms of flight time.

4.2.3.3 NO_x and CO_2 emissions

The NO_x and CO_2 emission models are presented in section 3.6. According to the results for this route, the total NO_x emission is 85.09 [kg] and the total CO_2 emission is 26644.87 [kg]. Briefly, the average NO_x and CO_2 emissions corresponds to in order of 7.74 [kg] and 2422.26 [kg]. Consequently, the average total aviation pollutants, NO_x and CO_2 emissions are examined within this study, has almost decreased by the numbers 22% and 9.9%.

5. CONCLUSION

The aircraft trajectory optimization is a continuously developing research field because of the economical and environmental concerns amongst aviation authorities. Fuel saving is a key factor to minimize carbon footprint within aviation and also to reduce operational costs.

This master thesis tackles the problem of aircraft trajectory optimization under wind effect by using optimal control techniques and focuses on environmental impact assessment. There are a number of operational constraints to improve safety in civil aviation from air traffic management perspective. Increasing air density associated with air traffic management restrictions, cause to diverge from optimality. For this reason by considering future aviation, the model is enhanced by assuming free route airspace. The aim of this study is to improve the impact of aviation on the environment. The multi-objective optimization problem in terms of fuel, travel time and NO_x emission costs has solved utilizing actual flight data. Cruise flight phase is critical part of a flight in terms of fuel consumption. Specifically, the numerical simulations are performed by modelling cruise stage.

Trajectory optimization had made by considering wind information to comply with real flights. However, because of the non-smoothness on wind tabular data, actual wind information was corrected and wind model has planned. In the simulation and results part, optimization results that have simulation environment prepared utilizing BADA 4 documents had shown, in order to achieve more accurate fuel consumption estimations. Artificial trajectories are planned with respect to the waypoints in the flight plan. In comparison between flown flight plan results and optimization results, as can be clearly seen in the application part, when the Istanbul-Ankara cruise phase is taken into account, thanks to the proposed model, an average of 6.8% fuel savings and a reduction in CO_2 emissions and at the same time a 15.87% reduction in NO_x emissions have been observed as well. As a second study, the proposed model was applied to a longer route by means of flight duration and distance. In European Airspace, Paris to Frankfurt flights investigated. The results show that fuel consumption and CO_2 emissions have reduced 9.9% and also approximately %22 decrement in NO_x emissions. Ultimately, this work is suitable for applying to the short-haul flights.

In the future, this study can be extended for intercontinental flights. Thus, the presented model can be validated for any type of flight. Additionally, the investigation can be improved by considering ATM restrictions and wind uncertainty. Understanding the behavior of the wind for planning future business trajectories is essential to increase realism. Wind information can be modelled with neural nets and the model with regression analyses and neural nets can be compared. Another critical issue for the future is aircraft noise, as indicated in "European Aviation Environmental Report 2019", noise can calculated by adding the noise indicator (L_{den}) to the objective function [1].

REFERENCES

[1] **EASA, EUROCONTROL,** (2019). European Aviation Environmental Report 2019.

[2] **Raptakis, A.** (2020). Optimization of Flight Trajectories of an Aircraft with respect to Fuel Consumption, MSc Thesis.

[3] **Delahaye, D., Legrand, K., Puechmorel, S., and Zhu, Y.** (2016). Aircraft trajectory planning under wind uncertainties, *IEEE/AIAA 35th Digital Avionics Systems Conference (DASC),* Sacramento, USA, pp.1-9.

[4] **Jensen, C.K., Chiarandini, M. and Larsen, K. (2017).** Flight Planning in Free Route Airspaces, *17th Workshop on Algorithmic Approaches for Transportation Modelling, Optimization, and Systems (ATMOS 2017),* Dagstuhl, Germany, pp. 1-14.

[5] **Legrand, K., Puechmorel, S., Delahaye, D. and Zhu, Y.** (2016). Aircraft trajectory planning under wind uncertainties, *IEEE/AIAA 35th Digital Avionics Systems Conference (DASC),* Sacramento, CA, USA , pp. 1-9.

[6] **Sridhar, B., Ng, H.K., Linke, F. and Chen, N.Y.** (2014). Benefits Analysis of Wind-Optimal Operations For Trans-Atlantic Flights, *14th AIAA Aviation Technology, Integration, and Operations Conference,* Atlanta, GA, pp. 1-12.

[7] **Zillies, J., Kuenz, A., Schmitt, A., Schwoch, G., Mollwitz, V. and Edinger, C.** (2014). Wind Optimized Routing: An Opportunity To Improve European Flight Efficiency, *2014 Integrated Communications, Navigation and Surveillance Conference (ICNS) Conference Proceedings,* Herndon, VA, USA, pp. X3-1-X3-9.

[8] **González-Arribas, D., Soler, M. and Sanjurjo-Rivo, M.** (2017). Robust Aircraft Trajectory Planning Under Wind Uncertainty Using Optimal Control, *Journal of Guidance, Control, and Dynamics*, 41(3), 673-688.

[9] **Zillies, J. L., Schmitt, A.R. and Vujasinovic, R.** (2013). Multiobjective 4D optimization of a trajectory-based air traffic management, *2013 Integrated Communications, Navigation and Surveillance Conference (ICNS),* Herndon, VA, USA, pp. 1-11.

[10] **Soler, M., Olivares, A. and Staffetti, E.** (2015). Multiphase Optimal Control Framework for Commercial Aircraft Four-Dimensional Flight-Planning Problems, *Journal of Aircraft*, 52(1), 274-286.

[11] **Lührs, B., Niklass, M., Froemming, C., Grewe, V. and Gollnick, V.** (2016). Cost-Benefit Assessment of 2D and 3D Climate And Weather Optimized Trajectories, *16th AIAA Aviation Technology, Integration, and Operations Conference*, Washington, D.C., pp. 1-14.

[12] **Soler, M., Zou, B. and Hansen, M.** (2014). Flight trajectory design in the presence of contrails: Application of a multiphase mixed-integer optimal control approach, *Transportation Research Part C: Emerging Technologies*, 48, 172–194.

[13] **Sridhar, B., Ng, H.K. and Chen, N.Y.** (2011). Aircraft Trajectory Optimization and Contrails Avoidance in the Presence of Winds, *Journal of Guidance, Control, and Dynamics*, 34(5), 1577-1584.

[14] **Lührs, B., Niklaß, M., Volker, G. and Gollnick, V.** (2018). Cost-Benefit Assessment of Climate and Weather Optimized Trajectories for Different North Atlantic Weather Patterns, *31st Congress of the International Council of the Aeronautical Sciences (ICAS)*, Belo Horizonte, Brazil, pp. 1-10.

[15] **Ng, H.K., Sridhar, B., Chen, N.Y. and Li, J.** (2014). Three-Dimensional Trajectory Design for Reducing Climate Impact of Trans-Atlantic Flights, 14th AIAA Aviation Technology, Integration, and Operations Conference, Atlanta, GA, pp. 1-12.

[16] **Matthes, S., Grewe, V., Dahlmann, K., Frömming, C., Irvine, E., Lim, L., Linke, F., Lührs, B., Owen, B., Shine, K., Stromatas, S., Yamashita, H. and Yin, F.** (2017). A Concept for Multi-Criteria Environmental Assessment of Aircraft Trajectories, *Aerospace*, 4, 42.

[17] **Bellman, R.** Dynamic Programming. Princeton UP, 1957.

[18] **Rao, A.** (2010). A Survey of Numerical Methods for Optimal Control, *Advances in the Astronautical Sciences*, 135.

[19] **Guijarro, R.A.** (2015). Commercial Aircraft Trajectory Optimization Using Optimal Control, *Bachelor Thesis*.

[20] **Nocedal, J. and Wright, S.** Numerical Optimization. Springer Verlag, 1999.

[21] **Cavcar, M.** (2017). The international standard atmosphere, *Elsevier*, 641-645.

[22] **Centre, E.E.** (2013). User Manual For The Base Of Aircraft Data (BADA) Revision 3.11, Technical Report.

[23] **Centre, E.E.** (2014). User Manual For The Base Of Aircraft Data (BADA) Family 4, Technical Report.

[24] **Başpınar, B., Balakrishnan, H. and Koyuncu E.** (2020). Optimization-Based Autonomous Air Traffic Control for Airspace Capacity Improvement, *IEEE Transactions on Aerospace and Electronic Systems*, 56(6), 4814-4830.

[25] **Opitz, H.C.** (2016). Prediction Method For Aircraft Landing System, PhD Thesis.

[26] **Nuic, A., Poles, D. and Mouillet, V.** (2010). BADA: An advanced aircraft performance model for present and future ATM systems, *International Journal of Adaptive Control and Signal Processing*, 24, 850-866.

[27] **Soler, M.** (2013). Commercial Aircraft Trajectory Planning based on Multiphase Mixed-Integer Optimal Control, PhD Thesis.

[28] **National Centers for Environmental Prediction, National Weather Service, NOAA, U.S. Department of Commerce.** (2015). NCEP GFS 0.25 Degree Global Forecast Grids Historical Archive, Research Data Archive at the National Center for Atmospheric Research, *Computational and Information Systems Laboratory*, https://doi.org/10.5065/D65D8PWK.

[29] **ICAO.** (2012). ICAO Engine Exhaust Emissions Data; Databank, Doc 9646-AN/943, Issue 18, ICAO: Montreal, QC, Canada, Available online: http://www.easa.europa.eu/document-library/icao-aircraft-engine-emissions-databank

[30] **DuBois, D., and Paynter, G.C.** (2006). Fuel Flow Method2 for Estimating Aircraft Emissions, *SAE Int.*, doi:10.4271/2006-01-1987.

[31] **Jelinik, F., Carlier, S., and Smith, J.** (2004). Advanced Emission Model (AEM3) v1.5, *Technical Report EEC/SEE/2004/004. Eurocontrol*, 306, 1–3.

[32] **Grobler, C., Wolfe, P., Dasadhikari, K., Dedoussi, I., Allroggen, F., Speth, R., Eastham, S., Agarwal, A., Staples, M., Sabnis, J. and Barrett, S.** (2019). Marginal climate and air quality costs of aviation emissions, *Environmental Research Letters*, 14, pp. 114031.

[33] **Beal, L. D. R., Hill, D. C., Martin, R. A. and Hedengren, J. D.** (2018). GEKKO Optimization Suite, *Processes*, 6(8), 106.

CURRICULUM VITAE

Name Surname : Fulin SEZENOĞLU

EDUCATION :

- **B.Sc.** : 2016, Bahçeşehir University, Faculty of Arts and Science, Department of Mathematics and Computer Science

PROFESSIONAL EXPERIENCE AND REWARDS:

- 2020-present, Research Assistant at Istanbul Technical University, Faculty of Aeronautics and Astronautics.

PUBLICATIONS, PRESENTATIONS AND PATENTS ON THE THESIS:

- **Sezenoğlu F.,** Başpınar B., and Özkol İ. 2022: Optimal Kontrol Teknikleri ile Rüzgar Etkisi Altında Uçak Rota Optimizasyonu. 9. Ulusal Havacılık ve Uzay Konferansı - Izmir University of Economics, September 14-16, 2022 İzmir, Turkey.